

## Synthesis and Characterization of Metal and Semiconductor Nanowires

Hardev Singh Virk

Professor Emeritus, Eternal University, Baru Sahib, HP, India  
hardevsingh.virk@gmail.com

**Keywords:** One-dimensional Nanomaterials, Anodic alumina & Polymer templates, Electrodeposition, VLS technique, Heterostructures, Semiconductor Nanowires, Laser ablation

**Abstract.** One-dimensional nanowires (NWs) have attracted considerable attention in recent years because of their novel physical properties and potential applications as interconnects in nanometre-scale electronics. NWs have potential applications in nanoscale electronics, optoelectronics, photonics, sensors, and solar cells due to their unique electrical, chemical, and optical properties. Several chemical and physical methods are commonly used to produce NWs. Among them, electrochemical synthesis and vapour-liquid-solid (VLS) methods to produce NWs have become popular among scientific workers due to a number of advantages. Synthesis of NWs using anodic alumina and polymer templates in an electrochemical cell has been described in detail as investigated in our laboratory. Characterization of metal and semiconductor NWs has been accomplished using scanning electron microscope (SEM), field emission scanning electron microscope (FESEM), high resolution transmission microscope (HRTEM), X-ray diffraction (XRD), and energy dispersive X-ray analysis (EDAX). Morphology of NWs has been revealed by SEM, structure by TEM, crystallinity by XRD and chemical composition by EDAX. I-V characteristics of copper and semiconductor NWs were recorded in-situ, as grown in pores of anodic alumina template, using Dual Source Meter (Keithley Model 4200 SCS) with platinum probes for contacts. Resonating tunneling diode (RTD) characteristics of fabricated NWs have been investigated. Bulk production of Copper NWs has been described by seed growth technique. Applications of NWs are not covered in any detail under this review.

### Table of Contents

1. Introduction
2. Synthesis Techniques of Nanowires (NWs)
  - 2.1 Template-assisted Synthesis
    - 2.1.1 Template Preparation
    - 2.1.2 Anodic Alumina Membrane (AAM) Fabrication
    - 2.1.3 Track-etched Polycarbonate (PC) Templates
    - 2.1.4 A variety of other Templates
  - 2.2 Electrochemical Deposition
    - 2.2.1 Methods for Improving the Quality of Nanowires
    - 2.3 Vapour-Liquid-Solid (VLS) Method for Nanowire Synthesis
    - 2.4 Other Synthesis Methods
3. Synthesis of Nanowires
  - 3.1 Fabrication of Metal Nanowires using Template-assisted Synthesis
  - 3.2 Synthesis of Semiconducting Nanowires
  - 3.3 Synthesis of Metal-Semiconductor Heterojunctions
4. Experimental Investigations and Characterization of Nanowires
  - 4.1 Characterization of Copper Metal Nanowires
    - 4.1.1 AFM, SEM and FESEM Analysis
    - 4.1.2 X-ray and EDAX Analysis
    - 4.1.3 I-V Characteristics of Copper Nanowires
  - 4.2 Chartacterization of Semiconductor Nanowires

4.2.1	Synthesis of CdS Nanowires
4.2.2	SEM, HRTEM and EDAX Analysis
4.2.3	I-V Characteristics of Cds Nanowires
4.3	Characterization of Metal-Semiconductor Heterojunctions
4.3.1	Synthesis of Cu-Se Nanowires
4.3.2	SEM, HRTEM and EDS Analysis
4.3.3	I-V characteristics of Cu-Se Heterostructures
5	Bulk Production of Copper Nanowires
6	Summary
	References

## 1. Introduction

In recent years, one of the most active areas of research has been nanotechnology [1-4]. The physical properties of nanomaterials are novel and completely different from those in conventional bulk materials. The new discovered properties of nanomaterials not only reflected in electronic transports but also exhibited in optics and magnetism. During last two decades, intensive and broad studies on nanoscience and nanotechnology were undertaken all over the world.

Quantum dots (0D), also known as nanocrystals, are a special class of materials known as semiconductors, which are crystals composed of periodic groups of II-VI, III-V, or IV-VI materials. They are so small, ranging from 2-10 nanometers (10-50 atoms) in diameter. At these small sizes materials behave differently, giving quantum dots/nanoparticles unprecedented tunability and enabling never before seen applications to science and technology. However, due to their small size and dispersed characteristic, only few limited applications have been developed, the examples are the quantum dots in matrix for opto-electronics, dispersed nanoparticles for drug carriers and thermal therapy of cancers etc. For above reasons, the study of nanowires stimulates a great interest in their fundamental scientific researches and potential applications.

One-dimensional nanowires (NWs) have attracted considerable attention in recent years [5-9] because of their novel physical properties and potential applications as interconnects in nanometre-scale electronics. The progress in this field has been accelerated by advances in both synthetic methods of preparing the nanoporous templates, and development of techniques capable of filling the pores of such membranes. Examples of high aspect ratio nanoporous membranes include nanochannel glass membranes, anodized aluminium substrates, and various polymeric membranes. Filling of the pores of such membranes with high aspect ratio nanowires/nanorods has been accomplished by electro-deposition, high-pressure metal melt injection, and photochemical methods.

Among various nanostructured materials, one-dimensional (1D) materials, such as nanowires, nanotubes, nanorods, and nanobelts, have potential applications in nanoscale electronics [10], optoelectronics [11], photonics [12, 13], sensors [14], and solar cells [15] due to their unique electrical, chemical, and optical properties [16-18]. Nanowires are useful in chemical or biological sensors for detecting single molecules because they have a high surface-to-volume ratio and a highly sensitive 1D nanostructure that gives rise to large conductivity change associated with binding molecules [14].

Nanowires, compared to other low dimensional systems, have two quantum confined directions, while still leaving one unconfined direction for electrical conduction. This allows nanowires to be used in applications where electrical conduction, rather than tunneling transport, is required. Because of their unique density of electronic states, nanowires in the limit of small diameters are expected to exhibit significantly different optical, electrical and magnetic properties from their bulk

3D crystalline counterparts. The increased surface area, very high density of electronic states, enhanced exciton binding energy, diameter-dependent band gap, and increased surface scattering for electrons and phonons are just some of the ways in which nanowires differ from their corresponding bulk materials. Synthesis, characterization and application of nanowires and nanotubes comprise a significant aspect of today's endeavor in nanotechnology [19, 20].

Our first introduction to nanowires happened through the use of heavy ion tracks recorded in dielectric films using heavy ion beam facility at GSI, Darmstadt. They offer unique possibilities for the realization of nanometer-sized structures at low cost and high throughputs [21-24]. In combination with lithography they open up new ways for biofluidic, electric, magnetic and optic device fabrication. Heavy ions produce along their path a nanometer channel of modified material with track diameter between 1 and 10 nm, adjustable by the chosen ion and its kinetic energy. The latent tracks created in irradiated materials may be used directly, e.g., creating conducting and magnetic nanowires in insulating matrices, or they may be selectively etched into pores and then used for nanobiofluidic applications, or as templates for growing micro/nanostructures. Commercial irradiation can produce ion track membranes with pore density ranging from single pore to  $10^8$  pores per  $\text{cm}^2$  per second.

## 2. Synthesis Techniques of Nanowires (NWs)

The synthesis of NWs has been studied extensively worldwide for a wide variety of materials. Several chemical and physical methods are commonly used to produce NWs. Among them, electrochemical synthesis or electrodeposition to produce NWs has a number of advantages, the most common being the controllability in the direction normal to the substrate surface. The length of the deposited NWs can be controlled by varying the duration of the electrodeposition process. In addition, electrochemical methods are inexpensive and operate at ambient temperatures and pressure. This chapter describes some methods of metal and semiconductor NWs production via electrochemical synthesis. Several electrochemical approaches have been reported to synthesize NWs including anodic aluminum oxide (AAO) template-assisted electrodeposition, lithographically patterned nanowire electrodeposition, surfactant-assisted electrodeposition, and template-free electrodeposition, etc. A great number of nanomaterials with diverse morphologies such as nanodots, nanoparticles, NWs, nanorods, nanobelts, nanotubes, nanospheres, nanoring, and nanoarrays, etc. have been synthesized based on template synthesis. All of these nanostructures were synthesized by deposition or growth of materials either inside the pores of the template or on the surface of the template. Among them the most popular technique is electrodeposition in the pores of AAO template, as it can stand high temperatures, is insoluble in organic solvents and geometrical parameters can be easily tuned by changing the synthesis conditions.

**2.1 Template-assisted Synthesis.** The template-assisted synthesis of nanowires is a conceptually simple and intuitive way to fabricate one-dimensional nanostructures [25-27]. These templates contain very small cylindrical pores or voids within the host material, and the empty spaces are filled with the chosen material, which adopts the pore morphology to form nanowires. In this section, we describe the templates first, and then describe strategies for filling the templates to make nanowires.

**2.1.1 Template Preparation.** In template-assisted synthesis of nanostructures, the chemical stability and mechanical properties of the template, as well as the diameter, uniformity and density of the pores are important characteristics to consider. Templates frequently used for nanowire synthesis include anodic alumina ( $\text{Al}_2\text{O}_3$ ), nano-channel glass, ion track-etched polymers and mica films. Porous anodic alumina templates are produced by anodizing pure Al films in various acids [28-30]. Under carefully chosen anodization conditions, the resulting oxide film possesses a regular hexagonal array of parallel and nearly cylindrical channels, as shown in Fig. 1(a, b). The self-organization of the pore structure in an anodic alumina template involves two coupled processes: pore formation with uniform diameters and pore ordering. The pores form with uniform diameters

because of a delicate balance between electric-field-enhanced diffusion which determines the growth rate of the alumina, and dissolution of the alumina into the acidic electrolyte [29]. The pores are believed to self-order because of mechanical stress at the aluminum-alumina interface due to expansion during the anodization. This stress produces a repulsive force between the pores, causing them to arrange in a hexagonal lattice [31]. Depending on the anodization conditions, the pore diameter can be systematically varied from <10 nm up to 200 nm with a pore density in the range of  $10^9$ - $10^{11}$  pores/cm<sup>2</sup> [28, 29, 32, 33]. It has been shown by many groups that the pore size distribution and the pore ordering of the anodic alumina templates can be significantly improved by a two-step anodization technique [34, 35], where the aluminum oxide layer is dissolved after the first anodization in an acidic solution followed by a second anodization under the same conditions.

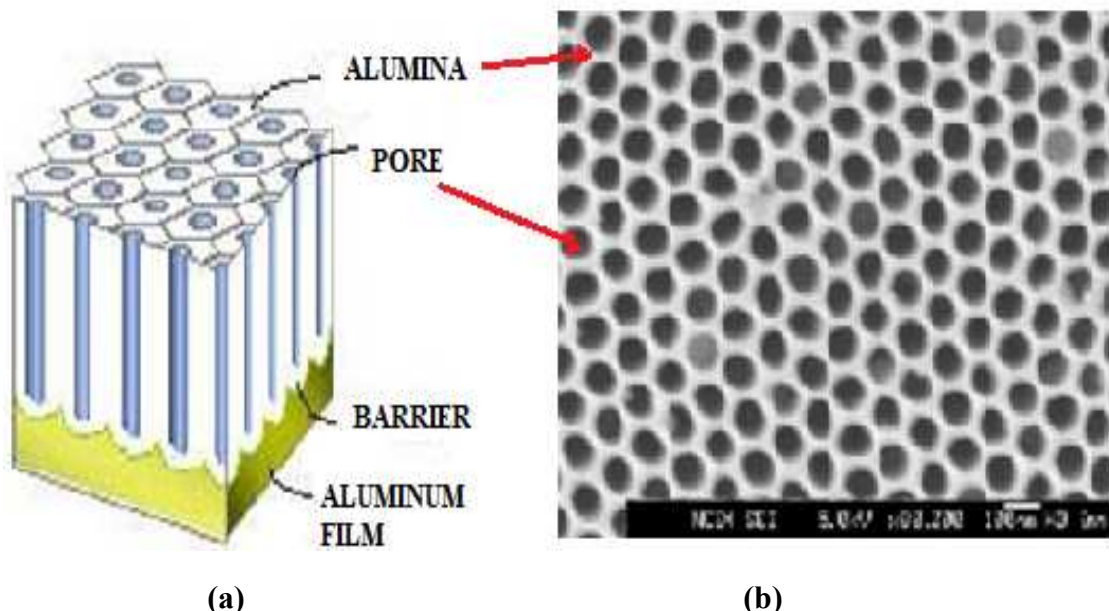


**Fig. 1(a, b)** Porous Anodic Alumina ( $\text{Al}_2\text{O}_3$ ) Template with hexagonal pores (T. Sands/ HEMI group <http://www.mse.berkeley.edu/groups/Sands/HEMI/nanoTE.html>)

Commercial templates are supplied with different pore sizes, pore density, diameter, thickness, and ready for use with or without pre-treatment by several companies. We used Whatman make anodic alumina templates (Fig. 2) for electrodeposition in our experiments [9].

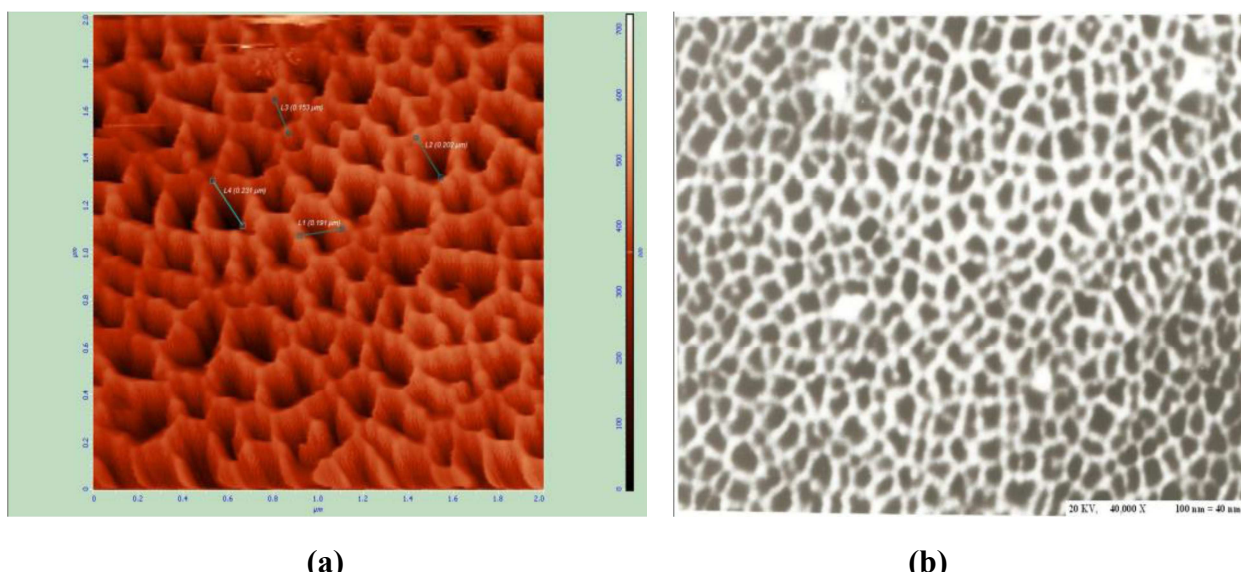


**Fig. 2 (a)** AFM image of hexagonal pores of commercial anodic alumina template (Whatman), **(b)** SEM image of the same after gold sputtering for use in electrodeposition [9]

**2.1.2 Anodic Alumina Membrane (AAM) Fabrication.** Commercial AAMs, having an average pore diameter varying from 20-200 nm, a nominal thickness of 60  $\mu\text{m}$  and a pore density of  $10^9$  pores/cm<sup>2</sup> are supplied by Whatman in the form of discs of varying diameters. These AAM discs are very fragile and need to be handled with care; otherwise cracks appear on the surface. The two-step anodization process is given as follows [35]: A pure Al sheet (99.997% purity, Vetec S.A.) was pretreated in a 5% NaOH solution at 60 °C for 60 seconds, neutralized in 1M HNO<sub>3</sub> for 30 seconds, washed in purified Milli-Q water and then etched in HNO<sub>3</sub>. The etched Al sheet was anodized at 10 Volt for 10 minutes and 15% H<sub>2</sub>SO<sub>4</sub> used as the electrolyte. The reaction products at anode and cathode were as described in eqns. 1 and 2, respectively.



The alumina oxide film (eqn. 1) was dissolved in 1% H<sub>3</sub>PO<sub>4</sub> at 60 °C for 20 minutes. The solution could completely dissolve the oxide film, but did not react with the Al substrate. The oxide dissolution in acid is given by eqn. (3):



The Al sheet was then re-anodized for 12 hours to create the desired long range ordering. The oxide film was removed in 1% H<sub>3</sub>PO<sub>4</sub> for 6 minutes and the desired AAM was obtained.

**2.1.3 Track-etched Polycarbonate (PC) Templates.** Another type of porous template that is commonly used for nanowire synthesis is the template fabricated by chemically etching particle tracks originating from ion bombardment [36], such as track-etched polycarbonate membranes (Fig. 3) [37-40]. We prepared our templates by using heavy ion beam irradiation of Makrofol-KG samples at GSI heavy ion linear accelerator, UNILAC, using <sup>132</sup>Xe (14.0 MeV/u) ion beams. All the irradiations were made at an angle of 90° with respect to the surface of the detector. The irradiated samples were cut into small pieces and etched in 6N NaOH solution at various temperatures, viz. 40, 50, 60 and 70 °C. The etched and dried samples were scanned under a Carl Zeiss optical microscope and the pore diameters were measured using a calibrated Filler eyepiece. The variation of pore diameter with etchant temperature was investigated. It was realized that chemical etching was not helpful in creating sub-micron size pores [21], for which we need electrolytically controlled etching.

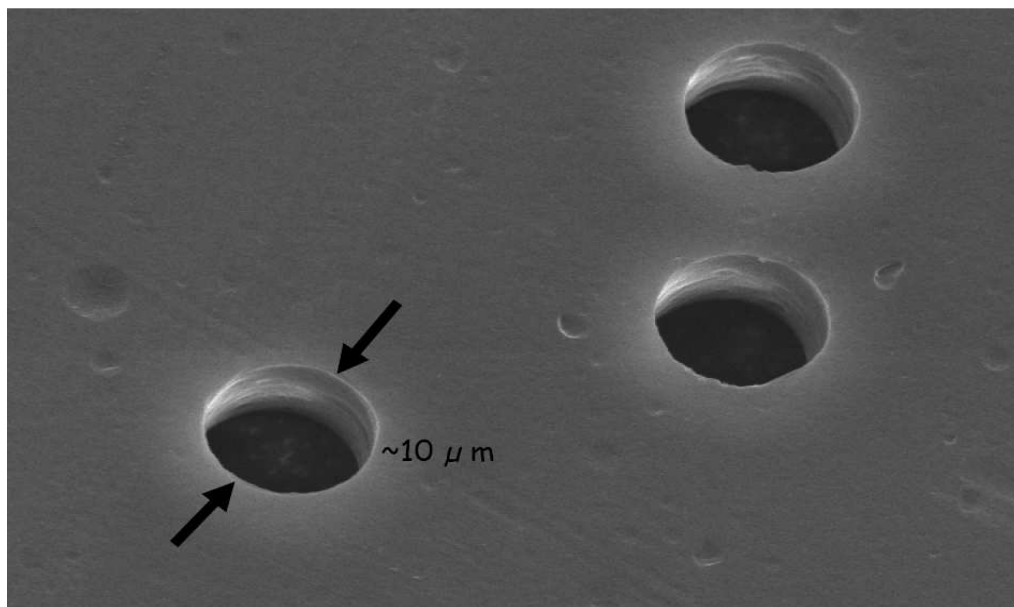


**Fig. 3** Ion track-etched polycarbonate membrane, each hole corresponding to exactly one etched latent track (<http://www.ion-tracks.de>)

A comparison of two types of templates, namely AAM and PC, is in order [20]. Both of these are very convenient to use during the growth of nanowires by various growth mechanisms, but each type of template also offers a few disadvantages. The advantage of using PC as the template is its easy handling and easy removal by means of pyrolysis at elevated temperatures, but the flexibility of PC is more prone to distortion during the heating process, and the removal of the template would occur before complete densification of the nanowires. These factors would result in broken and deformed nanowires. The advantage of using AAM as the template is its rigidity and resistance to high temperatures, allowing for the nanowires to densify completely before removal. This would result in a larger surface area of fairly free-standing and unidirectionally-aligned nanowire arrays. The problem with AAM is the complete removal of the template after nanowire growth, which has so far been unsuccessful using wet-chemical etching.

**2.1.4 A variety of other Templates.** Irradiated mica films have also been used as templates [41]. There are other porous materials that can be used as host templates for nanowire growth [25]. Nano-channel glass (NCG), for example, contains a regular hexagonal array of capillaries similar to the pore structure in anodic alumina with a packing density as high as  $3 \times 10^{10}$  pores/cm<sup>2</sup> [26]. Porous Vycor glass that contains an interconnected network of pores less than 10 nm diameter, was also employed for the early study of nanostructures [42]. Mesoporous molecular sieves [43], termed MCM-41, possess hexagonally-packed pores with very small channel diameters which can be varied between 2 nm and 10 nm. Conducting organic filaments have been fabricated in the nanochannels of MCM-41 [44]. Recently, the DNA molecule has also been used as a template for growing nanometer-sized wires [45]. Diblock copolymers, which consist of two different polymer chains with different properties, have also been utilized as templates for nanowire growth. When two components are immiscible in each other, phase segregation occurs, and depending on their volume ratio, spheres, cylinders and lamellae may self-assemble. To form self-assembled arrays of nanopores, copolymers composed of polystyrene and polymethylmethacrylate [P(S-b-MMA)] [46] were used. By application of an electric field while the copolymer was heated above the glass transition temperature of the two constituent polymers, the self-assembled cylinders of PMMA could be aligned with their main axis perpendicular to the film. Selective removal of the PMMA component afforded the preparation of 14-nm-diameter ordered pore arrays with a packing density of  $1.9 \times 10^{11}$  cm<sup>-3</sup>.

## 2.2 Electrochemical Deposition

The electrochemical deposition technique has attracted increasing attention as a promising alternative for fabricating nanowires. Traditionally, electrochemistry has been used to grow thin films on conducting surfaces. Since electrochemical growth is usually controllable in the direction normal to the substrate surface, this method can be readily extended to fabricate 1D nanostructures, if the deposition is confined within the pores of an appropriate template. In the electrochemical methods, a thin conducting metal film is first coated on one side of the porous membrane to serve as the cathode for electroplating. The length of the deposited nanowires can be controlled by varying the duration of the electroplating process. This method has been used to synthesize a wide variety of nanowires, e.g., metals {Bi [47]; Co [48-50]; Fe [32, 51]; Cu [52]; Ni [41, 48]; Ag [53]; Au [54]}; conducting polymers [38, 48]; superconductors {Pb [55]}; semiconductors {CdS [56]}; and even superlattice nanowires with A/B constituents, such as Cu/Co [57, 58], have been synthesized electrochemically.

In the electrochemical deposition process, the chosen template has to be chemically stable in the electrolyte during the electrolysis process. Cracks and defects in the templates are detrimental to the nanowire growth, since the deposition processes primarily occur in the more accessible cracks, leaving most of the nanopores unfilled. Particle track-etched mica films or polymer membranes are typical templates used in the simple *dc* electrolysis. To use anodic aluminum oxide films in the *dc* electrochemical deposition, the insulating barrier layer which separates the pores from the bottom

aluminum substrate has to be removed, and a metal film is then evaporated onto the back of the template membrane [59]. Compound nanowire arrays, such as  $\text{Bi}_2\text{Te}_3$ , have been fabricated in alumina templates with a high filling factor using the *dc* electrochemical deposition [60]. Figures 4(a) and (b), respectively, show the top view and cross-sectional SEM images of a  $\text{Bi}_2\text{Te}_3$  nanowire array [60].

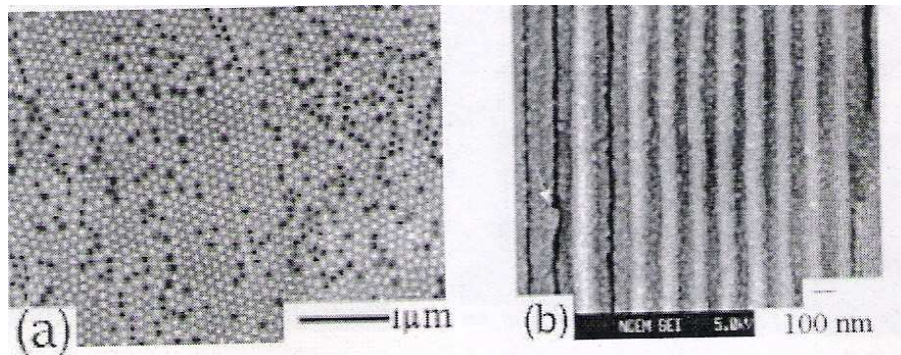


**Fig. 4** (a) SEM image of a  $\text{Bi}_2\text{Te}_3$  nanowire array top view, showing a high pore filling factor, (b) SEM image of nanowire array along the wire axis (adopted from ref. 60).

It is also possible to employ an *ac* electrodeposition method in anodic alumina templates without the removal of the barrier layer by utilizing the rectifying properties of the oxide barrier. In *ac* electrochemical deposition, although the applied voltage is sinusoidal and symmetric, the current is greater during the cathodic half-cycles, making deposition dominant over the etching, which occurs in the subsequent anodic half-cycles. Since no rectification occurs at defect sites, the deposition and etching rates are equal, and no material is deposited. Hence, the difficulties associated with cracks are avoided. In this fashion, metals, such as Co [50] and Fe [32, 51], and semiconductors, such as CdS [56], have been deposited into the pores of anodic aluminum oxide templates without removing the barrier layer. In contrast to nanowires synthesized by the pressure injection method, nanowires fabricated by the electrochemical process are usually polycrystalline, with no preferred crystal orientations, as observed by XRD studies. However, some exceptions exist. For example, polycrystalline CdS nanowires, fabricated by an *ac* electrodeposition method in anodic alumina templates [56], possibly have a preferred wire growth orientation along the c-axis. In addition, Xu et al. [61] have prepared a number of single-crystal II-VI semiconductor nanowires, including CdS, CdSe and CdTe, by *dc* electrochemical deposition in anodic alumina templates with a non-aqueous electrolyte [62]. Furthermore, single-crystal Pb nanowires can be formed by pulse electrodeposition under over-potential conditions, but no specific crystal orientation along the wire axis was observed [55]. The use of pulse currents is believed to be advantageous for the growth of crystalline wires because the metal ions in the solution can be regenerated between the electrical pulses and, therefore, uniform deposition conditions can be produced for each deposition pulse. Similarly, single crystal Ag nanowires were fabricated by pulsed electro-deposition [53].

Template synthesis by electrochemical deposition route is easy, low-cost as well as less cumbersome compared to other fabrication techniques, namely, pulsed laser deposition (PLD), vapour-liquid-solid (VLS) method and chemical vapour deposition (CVD). One advantage of the electrochemical deposition technique is the possibility of fabricating multi-layered structures within nanowires. By varying the cathodic potentials in the electrolyte which contains two different kinds of ions, different metal layers can be controllably deposited. In this fashion, Co/Cu multi-layered nanowires have been synthesized [57, 58]. Figure 5 shows TEM images of a single Co/Cu nanowire of about 40 nm in diameter [58]. The light bands represent Co-rich regions and the dark bands represent Cu-rich layers. This electrodeposition method provides a low-cost approach to prepare multi-layered 1D nanostructures.

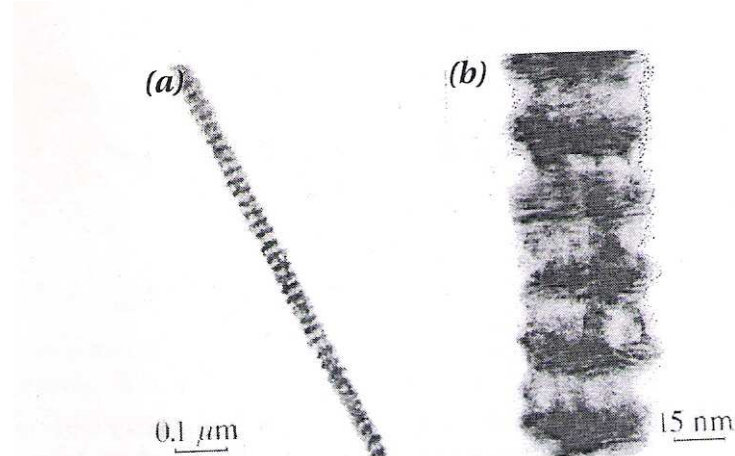


**Fig. 5** (a) TEM image of a single Co/ Cu multilayered nanowire, (b) a selected area of the sample at high magnification (adopted from ref. 58).

Template materials must meet certain requirements [5]. First, the template materials must be compatible with the processing conditions. For example, an electrical insulator is required for a template to be used in electrochemical deposition. Template materials should be chemically and thermally inert during the synthesis. Secondly, depositing materials or solution must wet the internal pore walls. Thirdly, for synthesis of nanowires, the deposition should start from the bottom of the template and proceed upwards to the other side. This is known as bottom up technique in nanotechnology.

Template-based synthesis offers many advantages over other methods of synthesis [63]: (1) It is performed under mild conditions rather than requiring high temperatures, high vacuum or expensive instrumentation; (2) templated electrodeposition has a relatively high growth rate; (3) the morphology of deposited materials depends on the shape of template pores; (4) the dimensions of the materials obtained can be tuned by tuning of the template pore size; (5) two or more components can be easily deposited into the membrane sequentially to form multi-segmented materials or hetero-junctions.

**2.2.1 Methods for Improving the Quality of Nanowires.** Despite manifold advantages of template-based synthesis, we may point out some major problems with this approach. It is relatively difficult to acquire densely continuous nanowires. This problem could be partially overcome by material injection at high pressure and high temperature [64]. The crystalline quality of nanowires needs improvement. Ying et al. [65] patented a technique to improve the control of crystalline quality, size, spacing and length of metal nanowires by pre-treating the pores. The pore wall can be modified to reduce the contact angle for complete filling by applying an acid solution, such as H<sub>2</sub>SO<sub>4</sub>. The thickness of the pore wall and composition of the pore surface can be varied and modified by vapor depositing a desired species. By using this technique, they obtained ultrafine Bi nanowires of good crystallinity, confirmed by XRD.

Another drawback of the template-assisted growth of nanowires is that the maximum nanowire length is limited by the thickness of the host template. Penner et al. [66] patented a method, called the step edge decoration technique, which has capability to synthesize long metallic nanowires (> 10 μm in length), uniform in diameter, and removable from the surface on which they are synthesized. The method starts with selective electrodeposition of metal oxide from an aqueous solution as a precursor, along step edges present on the stepped surface, such as graphite, to form a bead of metal oxide nuclei, which rapidly grow into hemi-cylindrical nanowires with continued deposition. Subsequently, metal nanowires are obtained from metal oxide nanowires by a reduction reaction in H<sub>2</sub> at 500 °C. Afterwards, polystyrene is cast into the gaps between nanowires to form a

nanowire/polystyrene film. Finally, the cast nanowire/polystyrene film is peeled off the graphite surface with the metal nanowire embedded therein. The entire process is represented by a sketch diagram (Fig. 6). Highly oriented pyrolytic graphite (HOPG) is the best available material used to grow  $\text{MoO}_2$  nanowires, which were reduced to free-standing metallic molybdenum nanowires by this method [67, 68].

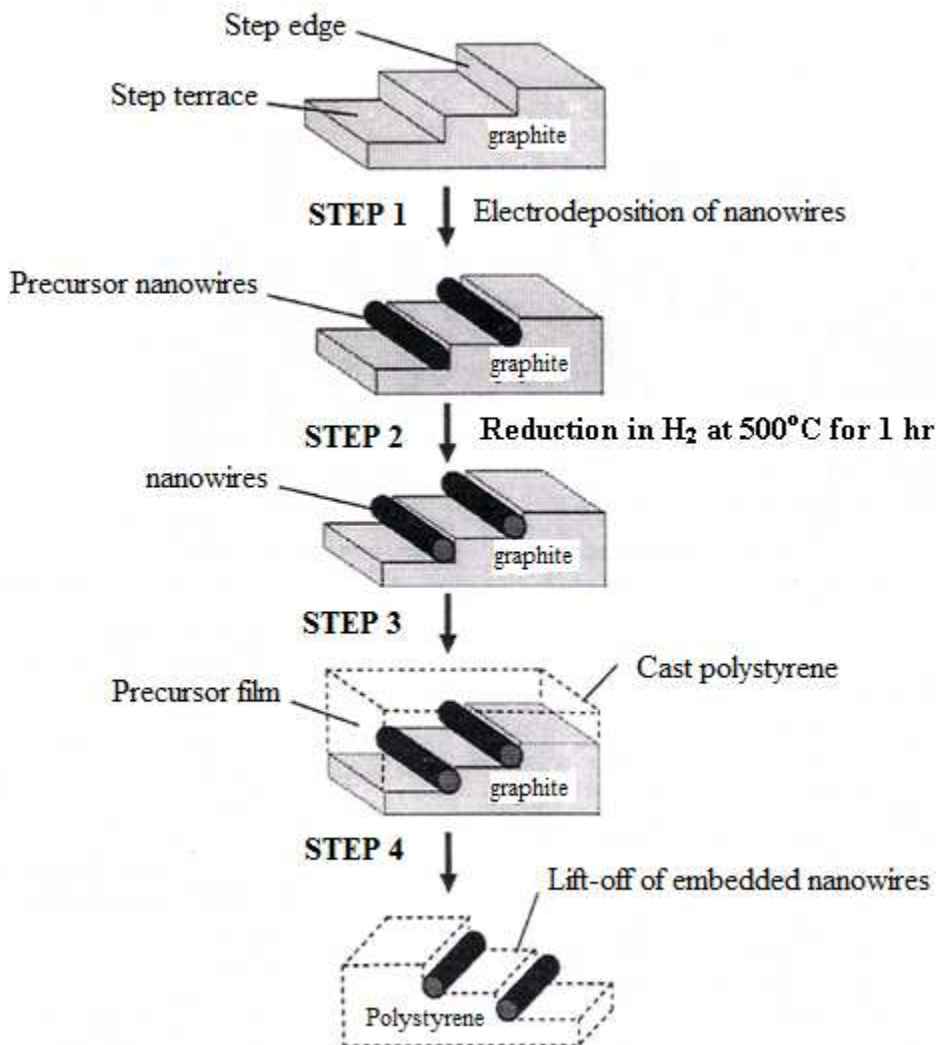


**Fig. 6** Schematic diagram for preparing long metallic nanowires by electrodeposition on the step edges of a stepped surface, such as graphite (adopted from ref. 66).

### 2.3 Vapour-Liquid-Solid (VLS) Method for Nanowire Synthesis

This method involves all three phases of matter, namely vapour, liquid and solid, hence popularly called VLS method. The process starts with the absorption of source material from the gaseous phase into a liquid droplet that acts as a catalyst. Primarily a liquid alloy is formed which becomes supersaturated and precipitates out the source material by nucleation. The precipitate acts as a preferred site for further deposition and growth of the material at the interface of the liquid droplet, favouring growth of the precipitate into a nanowire by suppressing further nucleation on the same catalyst.

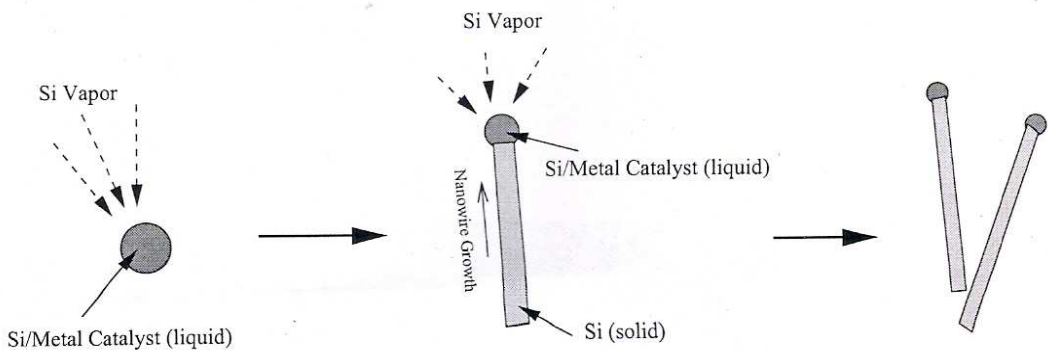


**Fig. 7** Schematic diagram illustrating the growth of Si nanowires by the VLS mechanism

Some of the recent successfully synthesized semiconductor nanowires are based on the so-called VLS mechanism of anisotropic crystal growth. This mechanism was first proposed by Wagner and Ellis [69] in 1964 for the growth of single crystal silicon whiskers 100 nm to hundreds of microns in diameter. The proposed growth mechanism (Fig. 7) involves the absorption of source material from the gas phase into a liquid droplet of catalyst (a molten particle of gold on a silicon substrate in the original work) [69]. Upon supersaturation of the liquid alloy, a nucleation event generates a solid precipitate of the source material. This seed serves as a preferred site for further deposition of material at the interface of the liquid droplet, promoting the elongation of the seed into a nanowire or a whisker, and suppressing further nucleation events on the same catalyst. Since the liquid droplet catalyzes the incorporation of material from the gas source to the growing crystal, the deposit grows anisotropically as a whisker whose diameter is dictated by the diameter of the liquid alloy droplet. The nanowires thus obtained are of high purity, except for the end containing the solidified catalyst as an alloy particle. Real-time observations of the alloying, nucleation, and elongation steps in the growth of germanium nanowires from gold nanoclusters by the VLS method were recorded by in-situ TEM [70].

Reduction of the average wire diameter to the nanometer scale requires the generation of nanosized catalyst droplets. However, due to the balance between the liquid-vapor surface free energy and the free energy of condensation, the size of a liquid droplet, in equilibrium with its vapor, is usually limited to the micrometer range. This obstacle was overcome in recent years by several new methodologies:

- (1) Advances in the synthesis of metal nanoclusters have made monodispersed nanoparticles commercially available. These can be dispersed on a solid substrate in high dilution so that when the temperature is raised above the melting point, the liquid clusters do not aggregate [71].
- (2) Alternatively, metal islands of nanoscale sizes can self-form when a strained thin layer is grown or heat treated on a non-epitaxial substrate [72].
- (3) Laser-assisted catalytic VLS growth is a method used to generate nanowires under non-equilibrium conditions. By laser ablation of a target containing both the catalyst and the source materials, a plasma is generated from which catalyst nanoclusters nucleate as the plasma cools down. Single crystal nanowires grow as long as the particle remains liquid [73].
- (4) Interestingly, by optimization of the material properties of the catalyst-nanowire system, conditions can be achieved for which nanocrystals nucleate in a liquid catalyst pool supersaturated with the nanowire material, migrate to the surface due to a large surface tension, and continue growing as nanowires perpendicular to the liquid surface [74]. In this case, supersaturated nanodroplets are sustained on the outer end of the nanowire due to the low solubility of the nanowire material in the liquid [75].

A wide variety of elemental, binary and compound semiconductor nanowires has been synthesized via the VLS method, and relatively good control over the nanowire diameter and its distribution has been achieved. Figure (8) shows the SEM image of ZnO nanowires grown by the VLS approach [76] using gold catalyst.

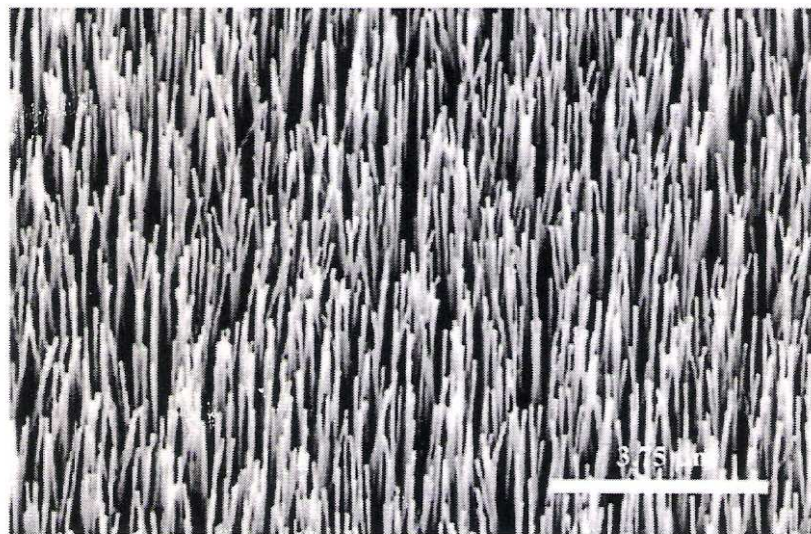


**Fig. 8** SEM image of the ZnO nanowires synthesized by VLS method using gold catalyst [76]

Researchers are currently focusing attention on the controlled variation of the materials properties along the nanowire axis. To this context, researchers have modified the VLS synthesis apparatus to generate compositionally-modulated nanowires. GaAs/GaP modulated nanowires have been synthesized by alternately ablating targets of the corresponding materials in the presence of gold nanoparticles [77]. The p-Si/n-Si nanowires were grown by chemical vapor deposition from alternating gaseous mixtures containing the appropriate dopant [77]. Si/Si<sub>1-x</sub>Ge<sub>x</sub> nanowires (Fig. 9b) were grown by combining silicon from a gaseous source with germanium from a periodically ablated target [78]. Finally, using an ultra-high vacuum chamber and molecular beams, InAs/InP nanowires with atomically sharp interfaces were obtained [79]. These compositionally-modulated nanowires are expected to exhibit exciting electronic, photonic, and thermoelectric properties.

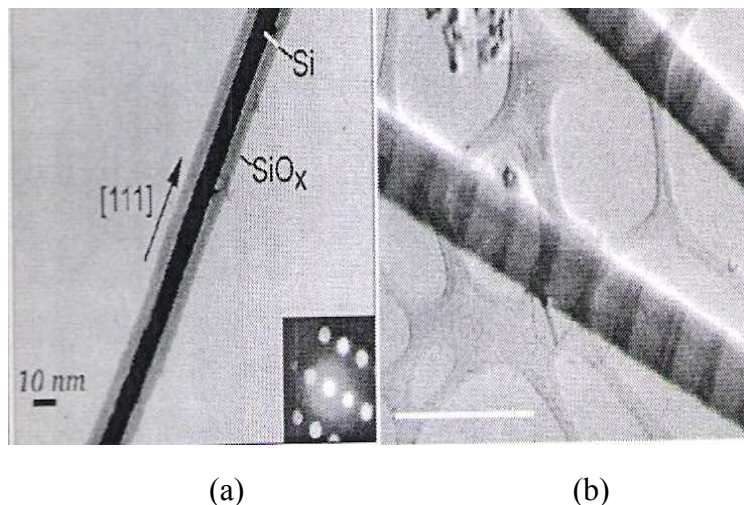


**Fig. 9** (a) Diffraction contrast TEM image of a Si nanowire showing crystalline Si core darker than the amorphous oxide surface layer [73], (b) STEM image of Si/Si-Ge superlattice nanowires in the bright field mode (scale bar is 500nm) [78].

Interestingly, silicon and germanium nanowires grown by the VLS method consist of a crystalline core coated by a relatively thick amorphous oxide layer (2-3 nm) (Fig. 9a). These layers are too thick to be the result of ambient oxidation, and it has been shown that these oxides play an important role in the nanowire growth process [80, 81]. Silicon oxides were found to serve as a special and highly selective catalyst that significantly enhances the yield of Si nanowires, without the need for metal catalyst particles [80-82]. A similar yield enhancement was also found in the

synthesis of Ge nanowires from the laser ablation of Ge powder mixed with  $\text{GeO}_2$  [83]. The Si and Ge nanowires produced from these metal-free targets generally grow along the [112] crystal direction [84], and have the benefit that no catalyst clusters are found on either ends of the nanowires. Based on these observations and other TEM studies [80, 83, 84], an oxide-enhanced nanowire growth mechanism different from the classical VLS mechanism was proposed, where no metal catalyst is required during the laser ablation-assisted synthesis (Fig. 10) [81]. It is postulated that the nanowire growth is dependent on the presence of  $\text{SiO}$  (or  $\text{GeO}$ ) vapor, which decomposes in the nanowire tip region into both Si (or Ge), which is incorporated into the crystalline phase, and  $\text{SiO}_2$  (or  $\text{GeO}_2$ ), which contributes to the outer coating. The initial nucleation events generate oxide-coated spherical nanocrystals. The [112] crystal faces have the fastest growth rate, and therefore the nanocrystals soon begin elongating along this direction to form one-dimensional nanostructures.

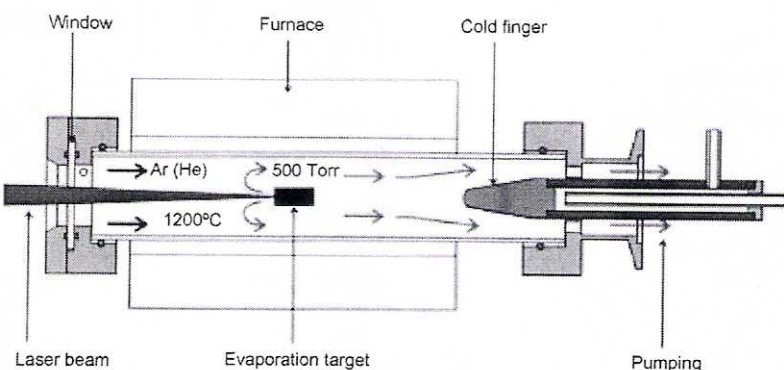


**Fig. 10** Experimental set up for the synthesis of Si nanowires by laser ablation method [81]

## 2.4 Other Synthesis Methods

In this section we review several other general procedures available for the synthesis of a variety of nanowires. We focus on “bottom-up” approaches, which afford many kinds of nanowires in large numbers, and do not require highly sophisticated equipment (such as scanning microscopy or lithography based methods), and exclude cases for which the nanowires are not self sustained (such as in the case of atomic rows on the surface of crystals). A solution-phase synthesis of nanowires with controllable diameters has been demonstrated [85, 86], without the use of templates, catalysts, or surfactants. Instead, Gates et al. [86] make use of the anisotropy of the crystal structure of trigonal selenium and tellurium, which can be viewed as rows of 1D helical atomic chain. Their approach is based on the mass transfer of atoms during an aging step from a high free-energy solid phase (e.g., amorphous selenium) to form a seed (e.g., trigonal selenium nanocrystal) which grows preferentially along one crystallographic axis. The lateral dimension of the seed, that dictates the diameter of the nanowire, can be controlled by the temperature of the nucleation step. Furthermore, Se/Te alloy nanowires were synthesized by this method [87], and  $\text{Ag}_2\text{Se}$  compound nanowires were obtained by treating selenium nanowires with  $\text{AgNO}_3$  [88, 89].

The pressure injection technique is often employed for fabricating highly crystalline nanowires from a low-melting point material or when using porous templates with robust mechanical strength. In the high-pressure injection method, the nanowires are formed by pressure injecting the desired material in liquid form into the evacuated pores of the template. Due to the heating and the pressurization processes, the templates used for the pressure injection method must be chemically stable and be able to maintain their structural integrity at high temperatures and at high pressures. Anodic aluminum oxide films and nano-channel glass are two typical materials used as templates in conjunction with the pressure injection filling technique. Metal nanowires (Bi, In, Sn, and Al) and semiconductor nanowires (Se, Te, GaSb, and  $\text{Bi}_2\text{Te}_3$ ) have been fabricated in anodic aluminum oxide templates using this method [90-91].

### 3. Synthesis of Nanowires

**3.1 Fabrication of Metal Nanowires using Template-assisted Synthesis.** A variety of metal nanowires, both single crystalline and polycrystalline in structure, have been fabricated using the electrodeposition technique, which is similar in principle to that used for the electroplating process. Copper is one of the most important metals in modern electronic technology. Keeping in view its role in nanoelectronics, we have fabricated copper nanowires of diameters 100 and 200 nm using anodic alumina and polymer membranes as templates [92, 93]. Many other groups [37, 39, 49, 94-96] have exploited this technique for synthesis of copper nanowires. Simultaneous production of Copper (Cu), Cuprous oxide ( $Cu_2O$ ) and Cupric oxide (CuO) nanowires have also been reported [97] and confirmed by XRD. Evidence for direct production of CuO and  $Cu_2O$  nanowires is also available [98, 99].

The template-assisted synthesis is a simple process. When an external electric field is applied between two dissimilar electrodes, charged species flow from one to another electrode, and electrochemical reactions occur at both electrodes. This process is called electrolysis, which converts electrical energy to chemical potential. The system used for the electrolysis process is called electrolytic cell. In such a system the electrode connected to the positive side of the power supply is an anode, at which an oxidation reaction takes place, whereas the electrode connected to the negative side of the power supply is a cathode, at which a reduction reaction proceeds, accompanied by deposition. Therefore, electrolytic deposition is also called cathode deposition, but most commonly referred to as electrochemical deposition or electrodeposition [20].

In our experiments, we used commercial anodic alumina membranes (AAM) (anodisc 25 made by Whatman, UK) having an average pore diameter of 200 nm, a nominal thickness of 60  $\mu m$  and a pore density of  $10^9$  pores/  $cm^2$ , as templates for synthesis of Copper nanowires. A second set of polymer membranes (Sterlitech, USA) of 100 nm pore diameter was selected for the sake of comparison. To achieve uniform deposition of nanowires, templates were cleaned in the ultrasonic bath for 10 minutes. The electrochemical cell, fabricated in our laboratory using Perspex sheets (Fig. 11), was washed in double distilled water. A copper rod of 0.8 cm diameter was used as a sacrificial electrode (anode). The cathode consists of copper foil attached to alumina disc by an adhesive tape of good conductivity. Prior to the electro-deposition process, a thin film of copper (0.5  $\mu m$ ) was sputtered onto one side of alumina disc. This metal layer along with adhesive copper tape provides a stable substrate (cathode) for the growth of nanowires. The electrolyte used had a composition of 20 gm/100ml  $CuSO_4 \cdot 5H_2O$  + 25% of dilute  $H_2SO_4$  at room temperature. A high concentration of  $CuSO_4$  was used to supply a sufficiently large number of ions inside the pores during the deposition. The electrodeposition was performed in the electrochemical cell at room temperature of 33  $^{\circ}C$ . Figure 12 illustrates the scheme of this process.



**Fig. 11** Electrochemical Cell, showing both the Cu electrodes jutting out of Perspex sheets

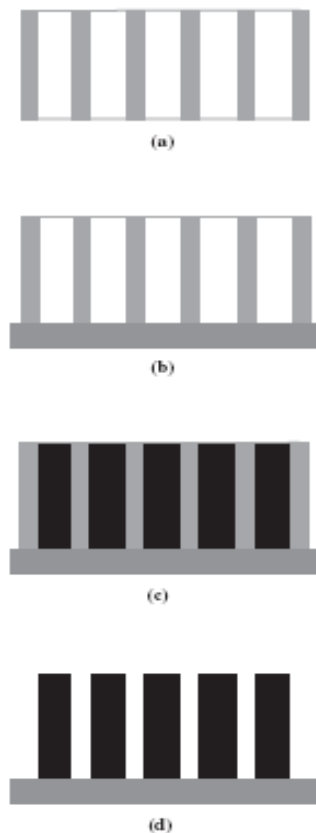


**Fig. 12** A schematic diagram of the template synthesis process (a) Anodic alumina template, (b) copper sputtered alumina template, (c) electrodeposited copper nanowires, and (d) copper nanowires after removal of anodic alumina template (adopted from ref. 97).

Polymer membranes can be prepared by irradiation of polycarbonate foils using heavy ion beams [37]. Author has prepared polymer templates, called Ion Track Filters [23], using Makrofol N and Kapton after irradiation at the UNILAC (Universal Linear Accelerator) of GSI, Darmstadt, with highly charged heavy ions having kinetic energies in the GeV range and fluences between  $10^6$  and

$10^{10}$  ions/cm<sup>2</sup>. Due to energy loss through interaction with the target electrons, each ion creates along its trajectory a cylindrical damage zone, a few nanometers in diameter. The damaged material can selectively be removed by controlled chemical etching, resulting in pores of cylindrical geometry. Composition, concentration, and temperature of the etching solution determine the size and geometry of the resulting pores, the pore diameter increasing linearly with the etching time. A 6 N NaOH solution containing 10% methanol at T = 50 °C was used for etching to produce pore diameters between 50 and 200 nm by varying time of etching. A thin gold film was sputtered onto one side of the membrane, using Jeol sputter JFC 1100 and reinforced by copper foil attached by an adhesive tape of good conductivity to obtain a stable substrate. This serves as a cathode suitable for the growth of the nanowires in polymer template in our two-electrode electrochemical cell. A schematic diagram of the polymer template synthesis process is illustrated in Figure 13 (a). Figure 13 (b) shows the geometry of polymer template pores of 100 nm diameter (Sterlitech USA) before electrodeposition.

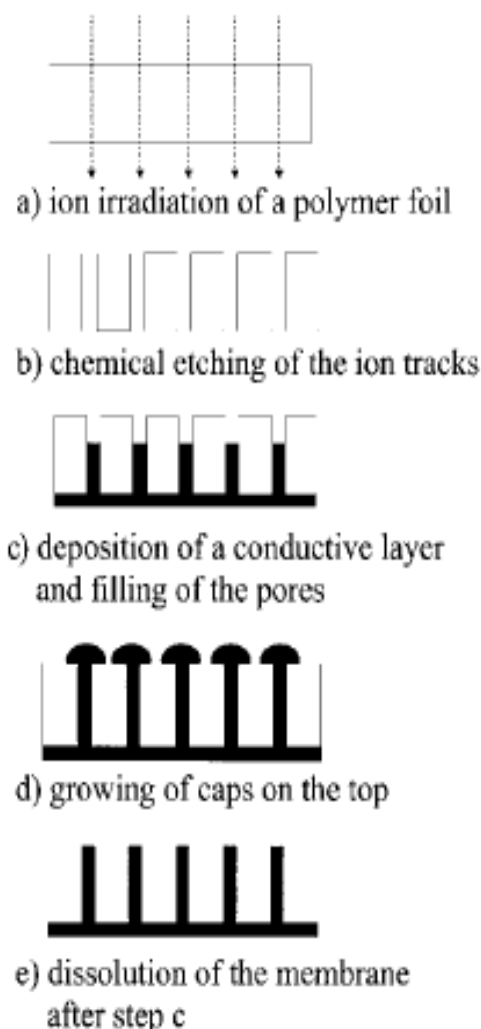


**Fig. 13 (a)** Scheme of polymer template synthesis of copper nanowires (adopted from ref. 37).

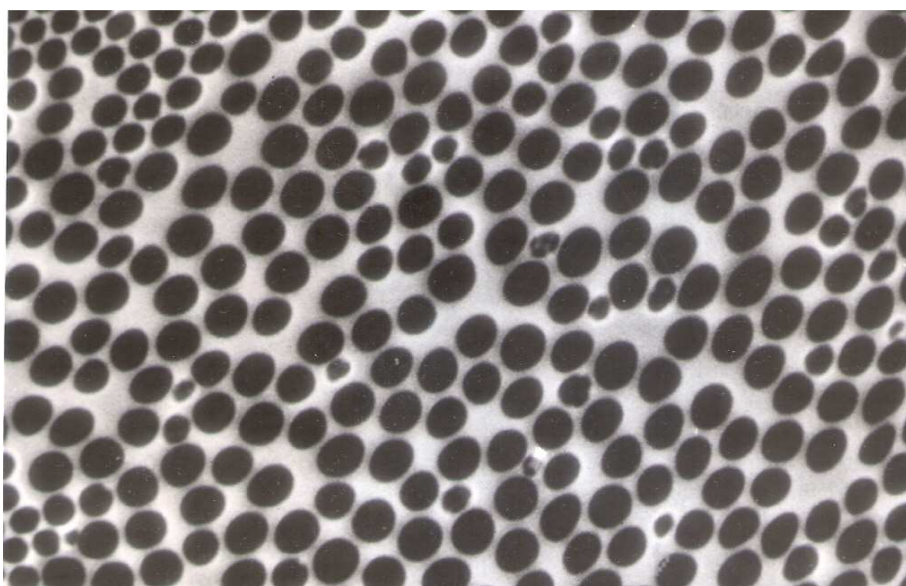


**Fig. 13 (b)** SEM micrograph of polymer template pores of 100 nm dia. before electrodeposition

The electrolyte used had a composition of 20 gm/100ml  $\text{CuSO}_4 \cdot 5\text{H}_2\text{O}$  + 25% of dilute  $\text{H}_2\text{SO}_4$  at room temperature. A high concentration of  $\text{CuSO}_4$  was used to supply a sufficiently large number of ions inside the pores during the deposition. Sulphuric acid was added to increase the conductivity of the solution and to lower the cathode over-voltage. The electrodeposition was performed at room temperature of 30 °C. The low over-voltages avoided side reactions such as hydrogen evolution. The inter-electrode distance was kept 0.5 cm and a current of 2mA was applied for 10 minutes using a regulated power supply. Electrodeposition of copper nanowires depends on many factors, namely, inter-electrode spacing, electrolyte composition, temperature and pH value, current density and time of deposition. The influence of current density, temperature and type of electrolyte on the crystallinity of copper nanowires has been reported elsewhere [37]. We studied the effect of current density on electrodeposition of copper nanowires in our experiment.

Template-assisted synthesis of Cu nanowires can be extended to other metals, provided we use an appropriate salt solution of the chosen metal as the electrolyte, a metal rod of appropriate dimensions as the anode and adopting the rest of the procedure same as for Cu nanowires. Schonenberger et al. [100] have synthesized Ni, Co, Cu, and Au, as well as polypyrrole polymer nanowires by template synthesis. Hamrakulov et al. [101] fabricated the Ni, Fe, Co and Cu single and multilayer nanowire arrays to make perpendicular magnetic recording media with nanoporous anodic alumina oxide (AAO) templates from Watt solution and additives by the *dc* electrodeposition. The results show that the diameters of Ni, Fe, Co and Cu single and multilayer nanowires in AAO templates are 40–80 nm and the lengths are about 30  $\mu\text{m}$  with the aspect ratio of 350–750 [101].

It has been reported [101] that Fe nanowires are deposited into the pores of the anodic alumina template by using a *dc* source. The electrolyte contained a large concentration of ferrous sulfate ( $\text{FeSO}_4 \cdot 7\text{H}_2\text{O}$ , 120 g/l;  $\text{H}_3\text{BO}_3$ , 45 g/l). Similarly, Co nanowires were fabricated from  $\text{CoSO}_4$  salt solution containing 40 g/l of  $\text{CoSO}_4 \cdot 7\text{H}_2\text{O}$  and 40 g/l of  $\text{H}_3\text{BO}_4$  as electrolyte [102]. In both the Fe and Co electro-deposition processes, *ac* voltage pulse of 10–20 V with frequency ranging from 50–300 Hz was used [103]. Cobalt nanowires have also been synthesized in polycarbonate templates at a constant *dc* potential in the range 1.20 - 1.25 V at room temperature (25 °C) using the same electrolyte as given above [104]. Ag nanowire arrays were prepared by chemical deposition [105] in an anodic alumina template using  $\text{AgNO}_3$  (20g/l) dissolved in glycol and followed by ultrasonic treatment for 1 minute, keeping the treated solution for 24h at 120 °C. It has also been reported [106] that by using highly concentrated electrolyte like 300 g/l  $\text{NiSO}_4 \cdot 6\text{H}_2\text{O}$  or 45 g/l  $\text{NiCl}_2 \cdot 6\text{H}_2\text{O}$

and 45 g of  $\text{H}_3\text{BO}_4$  solution of pH 4.5, Ni nanowires can be deposited into the pores of the alumina template under a negative current pulse of  $-25 \text{ mA/cm}^2$  for a duration of 6 minutes, followed by a positive voltage pulse of +4 V for 2 minutes only. Rahman et al. [107] prepared Ni nanowires in anodic alumina template by applying a constant current density of  $10 \text{ mA/cm}^2$  and using a mixture of 53.643g/l  $\text{NiSO}_4 \cdot 6\text{H}_2\text{O}$  and 30g/l  $\text{H}_3\text{BO}_3$  as electrolyte. Whitney et al. [108] synthesized Ni nanowires of 60 nm diameter in to a polycarbonate template using an electrochemical cell and plotted a current-time curve for the growth of nanowires (Fig. 14 b). They found that the current falls suddenly and reaches a plateau value when the deposition of Ni starts in the template pores; it rises as the deposition grows, and again reaches a plateau value when all the pores are filled up. Experimental set up for template-assisted growth of nanowires using an Electrochemical Cell with arrangement for anode, cathode, and porous membrane is shown in Fig. 14 (a).

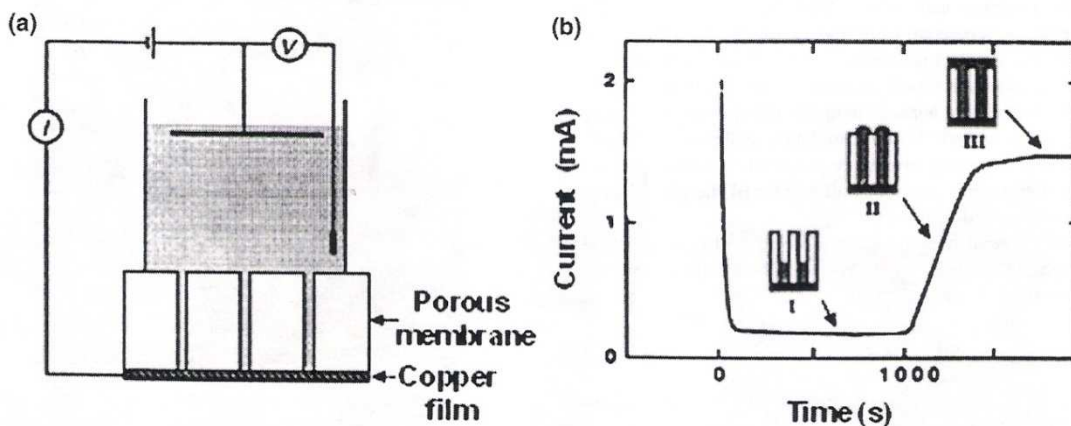


**Fig. 14** (a) Experimental set up for growth of nanowires in an electrochemical cell, (b) current-time curve for electrodeposition of Ni nanowires, showing different stages of the nanowire growth (adopted from ref. 20).

**3.2 Synthesis of Semiconducting Nanowires.** Single crystalline semiconductor nanowires (NWs) are being extensively investigated due to their unique electronic and optical properties and their potential use in novel electronic and photonic devices. Currently, tremendous efforts are being devoted to rational synthesis of semiconducting nanowire structures with control over their composition, structure, dopant concentration, characterization, fundamental properties, and assembly into functional devices. An exponential progress has been made in the area of nanowire optics and optoelectronic devices, including diodes, lasers, detectors, and waveguides. NWs synthesized from direct band gap semiconductors have shown tremendous potential for assembling nanophotonic devices for the generation, waveguiding, and detection of light at the nanoscale. A variety of semiconductor NWs have been fabricated using VLS and electrochemical deposition techniques from materials including  $\text{ZnO}$  [109],  $\text{ZnS}$  [110],  $\text{GaN}$  [111],  $\text{CdS}$  [56,112-117],  $\text{CdSe}$  [61,118-122],  $\text{CdO}$  [123],  $\text{ZnSe}$  [124],  $\text{InP}$  [125],  $\text{GaAs}$  [126], and  $\text{Se}$  [127].

Semi-conducting  $\text{ZnO}$  NWs are finding applications in solar cells.  $\text{ZnO}$  is a direct wide band gap semiconductor ( $E_g = 3.4 \text{ eV}$ ) with large exciton binding energy ( $\sim 60 \text{ meV}$ ), suggesting that it is a promising candidate for stable room temperature luminescent and lasing devices. Compared with  $\text{TiO}_2$ ,  $\text{ZnO}$  shows higher electron mobility with similar band gap and conduction band energies. Therefore,  $\text{ZnO}$  nanowires can be used as an alternative candidate for high efficiency solar cells. Chao et al. [128] reported that the  $\text{ZnO}$  NWs were grown in a furnace by chemical vapor deposition (CVD) with gold as catalyst. SEM image of aligned  $\text{ZnO}$  NW arrays (Fig. 15) on the sapphire substrate resembles with the SEM image of  $\text{ZnO}$  NWs grown by VLS method (Fig. 8). This image revealed that the  $\text{ZnO}$  wires are vertically aligned, the length of nanowires is around 1-2 mm and the diameter is in the range of 70-100 nm.

Because chemical and physical vapor deposition need to work in vacuum and/or at high temperature, these techniques require sophisticated and expensive equipments. The electrochemical deposition technique is becoming an important means for the fabrication of ZnO NWs due to the low cost, mild conditions, accurate process control and its being widely used in industry. Leprince-Wang et al. [129] reported on the structure study of ZnO NWs grown via electrochemical deposition, a simple and low temperature approach. Figure 16 presents a typical TEM image showing the general morphology of the electrodeposited ZnO NWs. It is found that the nanowires formed from the M90 type membrane are about 130-150 nm in diameter and 2-3 mm in length.

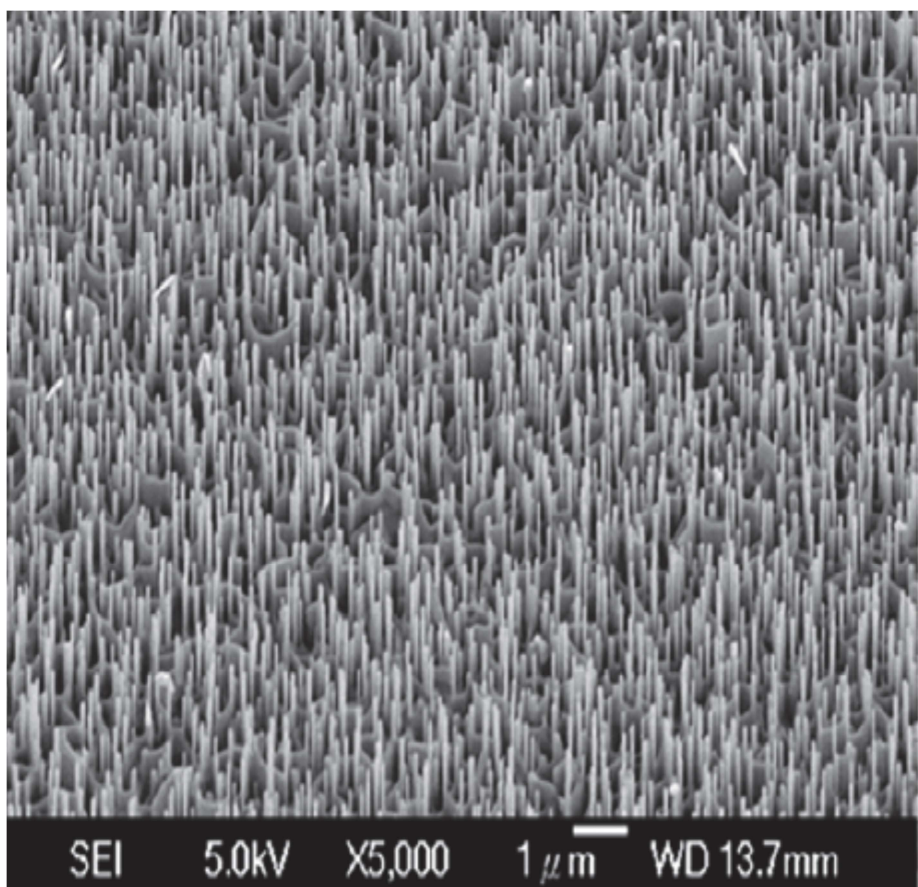


**Fig. 15** SEM image of aligned ZnO nanowire arrays grown by CVD (adopted from ref.128)

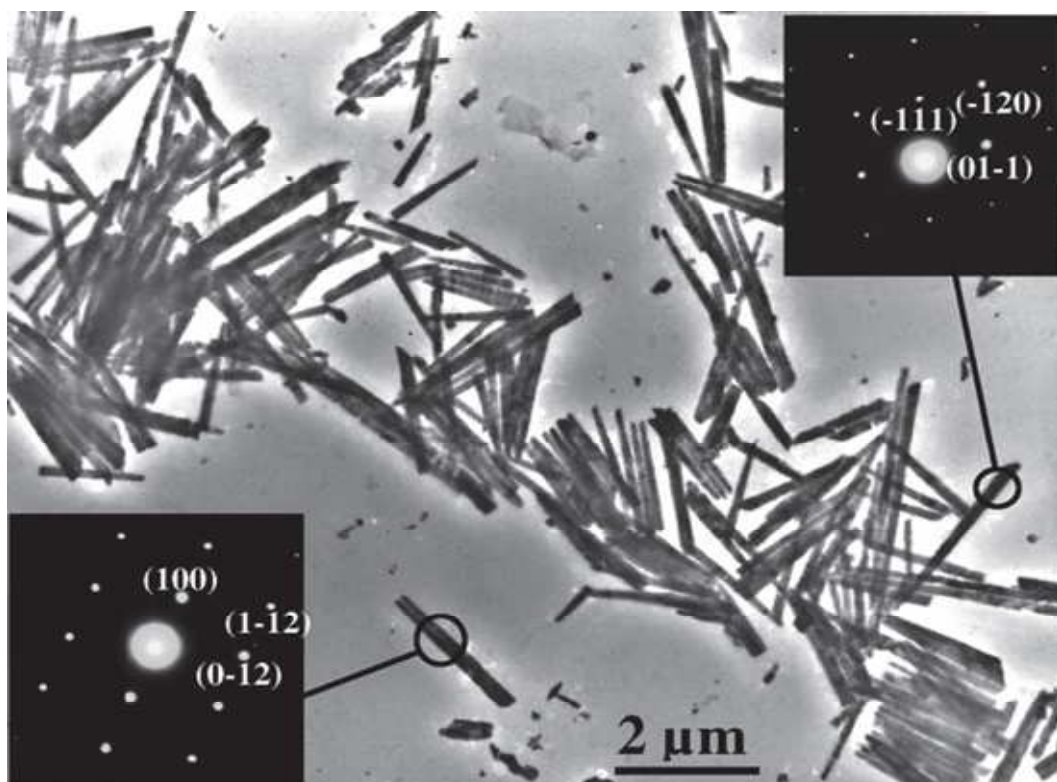


**Fig. 16** TEM image showing a general morphology of the electrodeposited ZnO nanowires (adopted from ref. 129).

**3.3 Synthesis of Metal-Semiconductor Heterojunctions.** Metal-semiconductor interfaces lead to development of heterojunction structures and devices like Schottky barrier diodes, resonant tunneling diodes (RTDs), bipolar transistors, superlattices, quantum wells, nanowires and quantum dots. RTD is a device that exhibits a negative differential resistance in its I-V characteristics due to quantum mechanical tunneling phenomenon and has a wide variety of ultra-high speed applications for electronic circuits. These include their use as terahertz oscillators, memories, electro-absorption modulators, and analog to digital converters.

Cu-Se heterostructure NWs have been synthesized by using polycarbonate track-etched membranes (TEM) with pore diameters varying from 100 nm to 2  $\mu\text{m}$  [130-132]. The cell used for electro-deposition of Cu-Se heterostructures had conducting copper tape attached to TEM, which served as the cathode, and the anode consisted of a pure copper sheet. The electrolyte used had a composition of  $\text{CuSO}_4 \cdot \text{H}_2\text{O}$  (200 gm/l) + dilute  $\text{H}_2\text{SO}_4$  (20g/l) at room temperature of 25  $^{\circ}\text{C}$ , and a potential difference of 2V (current variation 0.019 to 0.025 A) was applied for 10 minutes using a *dc* source. When the TEM pores were approximately half-filled up with copper metal, the electrolyte was drained out and a second electrolyte having a composition of  $\text{SeO}_2$  ( $9 \times 10^{-4}$  M) with 0.5 ml of dilute  $\text{H}_2\text{SO}_4$  was introduced in the cell. A potential difference of 3V (current variation 0.020 to 0.025) was applied for 12 minutes at 60 $^{\circ}\text{C}$  to electro-deposit Se semiconductor over Cu metal already deposited in TEM pores. Subsequently, the electro-deposited sample was removed from the cell, washed and dried for 30 minutes, and the TEM was dissolved in dichloromethane ( $\text{CH}_2\text{Cl}_2$ ) to liberate NWs. Figure 17 shows the schematic diagram of the fabrication process of Cu-Se heterostructure NWs.

I-V characteristics of the Cu-Se NWs show some interesting features (Fig. 18). RTD behavior is shown by NWs of 100 nm diameter at annealing temperatures above the room temperature, and the bulk behavior by 2  $\mu\text{m}$  diameter NWs. It clearly shows that quantum size effects disappear for thick

NWs. Virk [133] observed p-n junction diode behavior instead of RTD for Cu-Se NWs fabricated by electro-deposition using anodic alumina template in lieu of TEM.

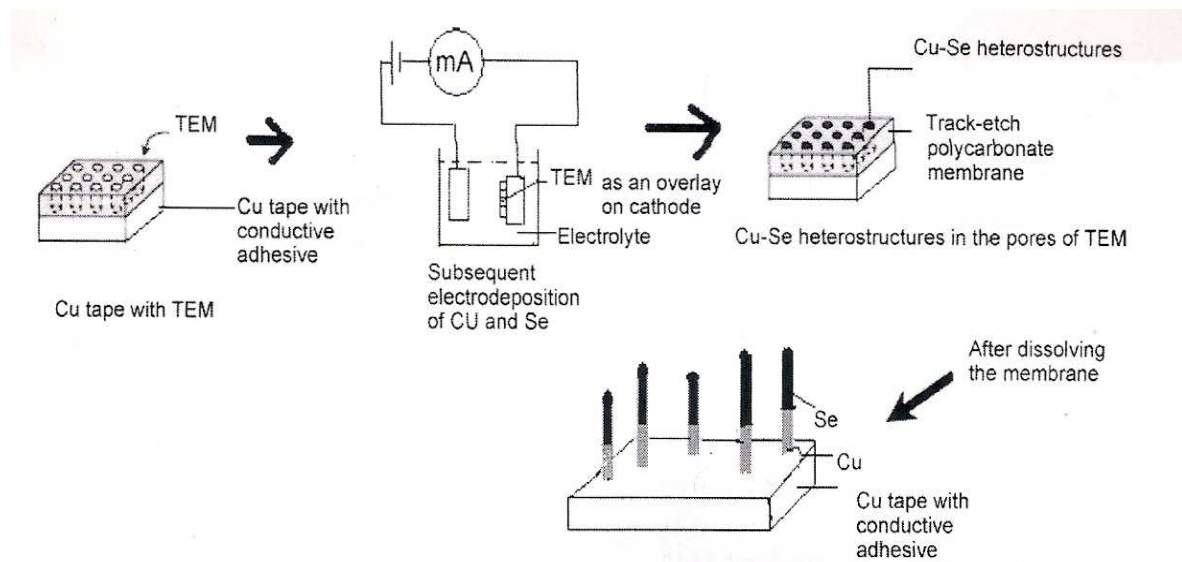


**Fig. 17** The schematic diagram of the fabrication process of Cu-Se nano/micro heterostructures using track-etched membrane (TEM) (adopted from ref. 132).

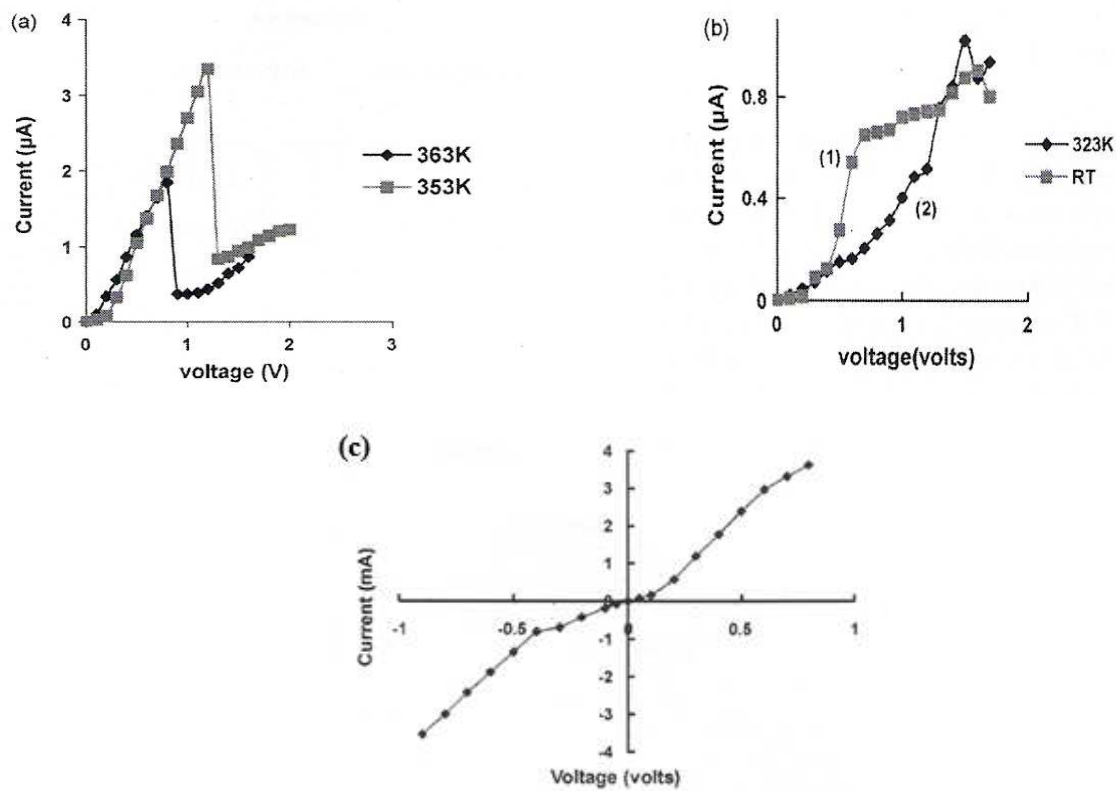


**Fig. 18** (a, b) I-V plots of Cu-Se nanowires of 100 nm diameter at different annealing temperatures showing RTD behavior, (c) I-V characteristics of Cu-Se nanowires of 2 μm diameter showing bulk behavior (adopted from ref. 132).

Zn-Se heterojunction arrays were fabricated by electrochemical deposition in the nanoporous track-etched membrane using an aqueous solution of 0.5 ZnSO<sub>4</sub> and 10<sup>-4</sup>M SeO<sub>2</sub> (pH=2.4) at 60 °C as an electrolyte. I-V characteristics reveal RTD behavior of Zn-Se NWs [134]. Following the same fabrication route, Zn-Se and Cd-Se heterojunctions have been studied and RTD behavior confirmed

by experiments [135]. RTD behavior inside semiconductor NW heterostructures has been studied by Bjork et al. [136]. It is predicted that such structures would be of great value for nanoelectronic devices and for basic research. Co-Pb NW arrays were fabricated in anodic alumina templates to investigate the magnetic properties of these nanowires [137]. Alloy nanowires of Ni-Fe-Co were synthesized by electrodeposition in modified anodic alumina template by Saedi and Ghorbani [138].

#### 4.0 Experimental Investigations and Characterization of Nanowires

##### 4.1 Characterization of Copper Metal Nanowires

**4.1.1 AFM, SEM and FESEM Analysis.** Commercial available templates (Whatman anodisc) were examined before their use using Atomic Force Microscope (NT-MDT PR 400 Model) installed in our laboratory and Scanning Electron Microscope (Jeol, JSM 6100) facility of Punjab University, Chandigarh. Atomic force microscopic technique [139] shows the two dimensional surface topology of the anodic alumina membrane (AAM) template with hexagonal pores regularly arranged on the surface (Fig. 2a). The pores appear nearly at the centre of each hexagonal cell. After gold sputtering, using Jeol sputter JFC 1100, SEM micrograph (Fig. 2b) shows the geometrical pattern of pores on the alumina surface of anodisc.

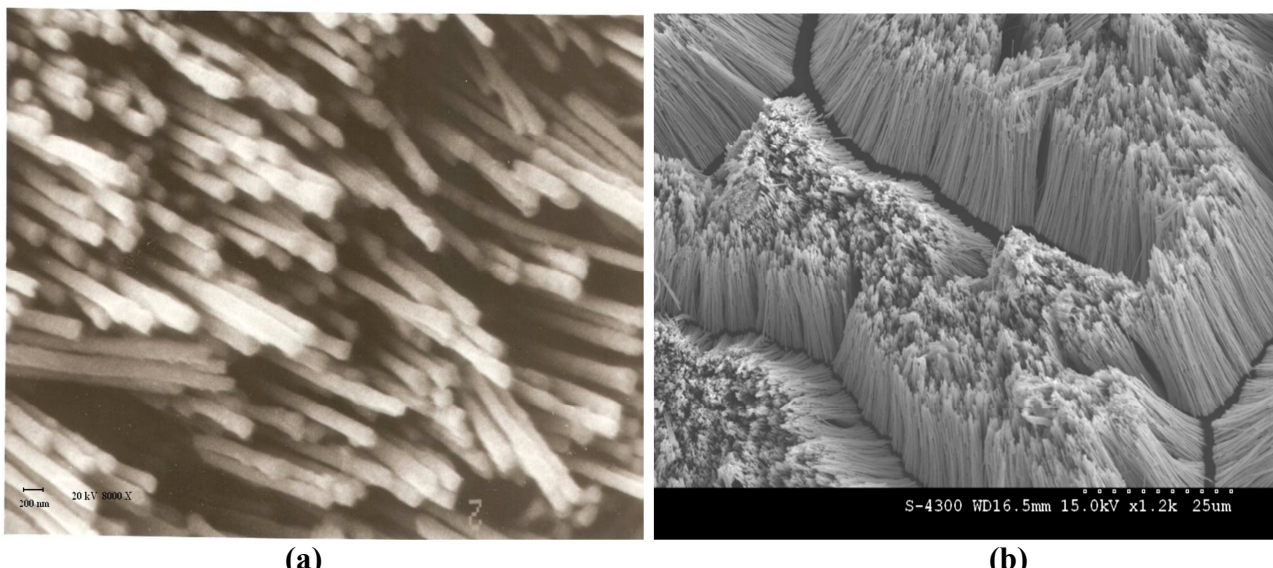


**Fig. 19** SEM images of copper nanowires of 200 nm diameter (cross-sectional and top views)

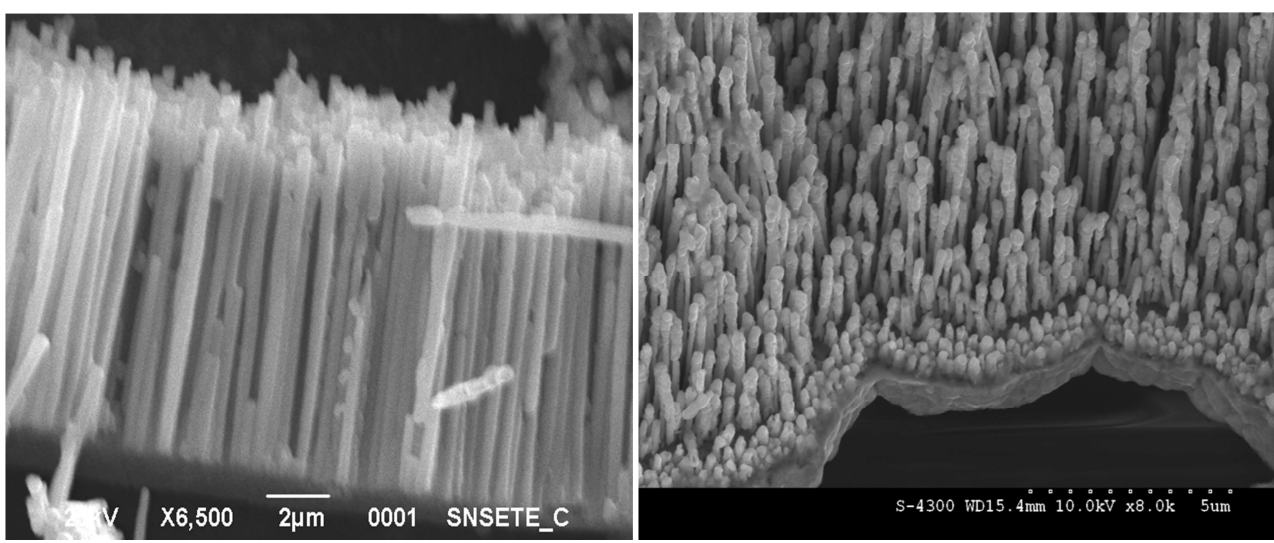


**Fig. 20 (a)** SEM image of copper nanowires fabricated under constant current (lateral view),  
**(b)** SEM image of copper nanowires fabricated under transient current and showing capping effect

The details of fabrication of Cu nanowires by electrodeposition are already given in Section 3.1. AAM with embedded Cu nanowires was kept immersed in 1 M NaOH for 3 hours in a beaker to dissolve alumina template. The copper nanowires were liberated from the host matrix, washed in distilled water and dried in an oven at 50 °C for 30 minutes. The cleaned and dried nanowires were mounted on aluminium stubs with the help of double adhesive tape, sputtered with a layer of gold using Jeol sputter JFC 1100. SEM (Jeol, JSM 6100) was used to record cross-sectional and lateral views of grown nanowires at an accelerating voltage of 20kV using different magnifications. SEM images (Fig. 19) show the cross-sectional and top view of copper nanowires of 200 nm diameter grown in alumina template, respectively. It has been observed that the cracks along the AAM facilitate the growth of bundles of nanowires during the electrodeposition process (Fig. 19b).

Two sets of templates were used for the growth of copper nanowires. In one set, current density was kept constant and in the other, it was changed intermittently which resulted in non-uniform growth of nanowires. Figure 20(a) shows the SEM image of copper nanowires array in lateral view, grown under constant current conditions. Figure 20(b) represents the FESEM image of copper nanowires fabricated under transient current conditions. Overdeposition of copper is clearly visible towards the tip of nanowires resulting in capping effect. Nanowires are quite uniform with diameter in the range of 200 nm but they are not perfect cylinders. It has been reported [100] that pore diameters of commercially available templates vary over a large range. The aspect ratio, that is, the ratio of length to diameter, is on the order of 300.

The experiment was repeated using the same electrochemical cell but substituting anodic alumina membrane by the polycarbonate membrane with pore diameter of 100 nm as a template and keeping the other conditions identical. However, we failed to sputter thin copper film onto one side of the membrane, as the polymer template failed to withstand the high temperature inside the vacuum coating unit. The experiment was performed with bare polymer template pressed on to the copper foil, acting as the cathode. After electrodeposition, the polymer template was dissolved in dichloromethane to liberate copper nanowires from the host matrix. The rest of the procedure is same. SEM micrographs of grown copper nanowires are shown in Fig. 21(a, b). The cross-sectional and lateral views are somewhat distorted and not as smooth as in the case of AAM templates. The diameter of copper nanowires matches with the pore diameter (100 nm) of polycarbonate template.

We repeated the experiment for 20 nm pore diameter polycarbonate template. The template was used as such and not coated with a conducting layer during electrodeposition. It resulted in failure to grow nanowires but the failure of experiment proved to be a blessing in disguise. Instead of copper nanowires, we observed growth of double pyramid shaped copper crystals (Fig. 22). We could not find any evidence for this phenomenon in literature. It is anticipated that copper ions from the electrolyte do not enter template pores due to poor conductivity but get deposited on the cathode surface in the form of polycrystalline crystals. Polycrystalline nature of Cu crystals was confirmed by XRD.

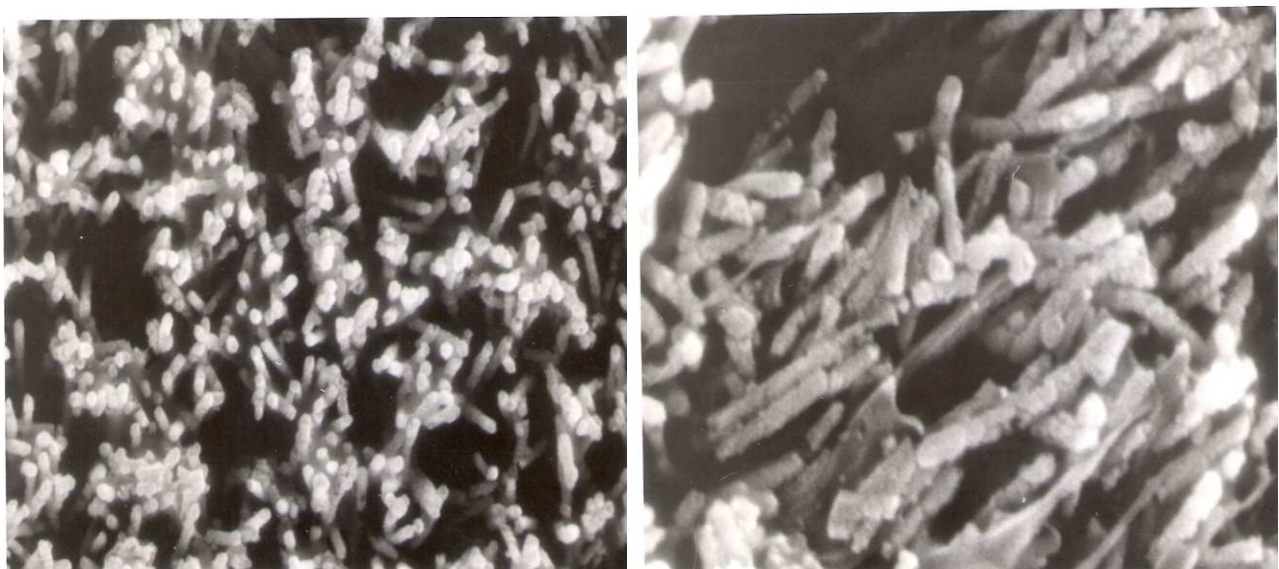


**Fig. 21** SEM images of Cu nanowires (100 nm dia.) grown in polymer template showing  
(a) cross-sectional and (b) lateral views

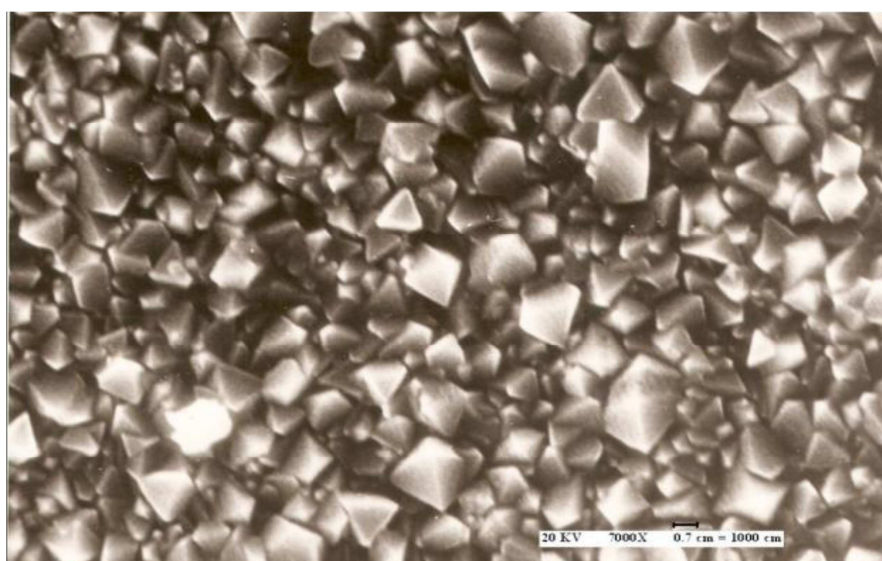


**Fig. 22** SEM micrograph of double pyramid shaped polycrystalline copper crystals grown on polymer template

**4.1.2 X-ray and EDAX Analysis.** The characterization techniques that are commonly used to study the crystal structure and chemical composition of nanowires include X-ray diffraction and energy dispersion X-ray analysis (EDAX). Both these techniques have been employed in our analysis.

The crystal structure of the double pyramid shaped copper crystals has been determined using X-ray diffraction analysis. XRD spectrum (Fig. 23) shows two prominent peaks corresponding to  $2\theta = 43.4610$  and  $50.5803$ , with  $d$  spacing = 2.082 and 1.804, respectively. These peaks reveal the polycrystalline nature of copper crystals, indicating that preferred growth direction of crystals is the (200) plane. Template based synthesis of single crystal copper nanowires has been reported in literature [37, 49, 97] with preferred growth direction along (111) plane, but to the best of our knowledge, there is hardly any report for growth of copper crystals or copper nanowire arrays with a (200) preferred orientation.

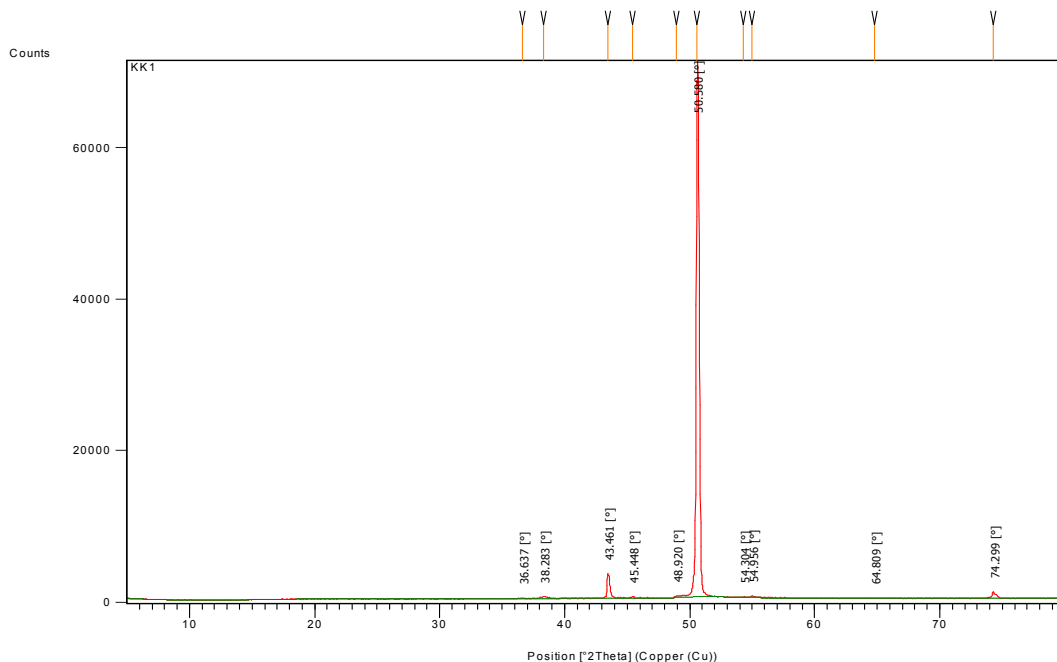


**Fig. 23** XRD spectrum of pyramid shaped polycrystalline copper crystals

The crystallographic structure of copper nanowire arrays was investigated by X-ray diffraction analysis (XRD). For sake of comparison, XRD spectrum of Cu foil used as a substrate (cathode) was also recorded (Fig. 24). XRD diffractograms were obtained in the  $2\theta$  range from  $10^0$  to  $80^0$  with a step of  $0.02^0$ , using the Cu K $\alpha$  radiation source of  $\lambda = 1.5406 \text{ \AA}$ . XRD spectrum (Table 1) shows three prominent peaks corresponding to  $2\theta = 43.5966, 50.8127$  and  $74.4331$ , with d spacing = 2.074, 1.80 and 1.27, and corresponding Miller indices, (111), (200) and (220), respectively. All peaks can be attributed to the crystalline cubic form of metallic copper [7]. XRD spectrum of copper nanowires (Fig. 25) shows some interesting results. There are in all 8 peaks in the spectrum; with 2 additional peaks at  $2\theta = 37.0062$  and  $54.9761$ , which are of negligible intensity and may be ignored. Three main peaks are also there (Fig. 24) but two of them split into double and triple peaks (Table 2), which may be attributed to X-ray scattering at the substrate. These peaks reveal the polycrystalline nature of copper nanowires, the most prominent peak at  $2\theta = 50.9870$ , indicating that the preferred growth direction of nanowires is the (200) plane. Due to polycrystalline nature of copper nanowires, the most prominent peak at  $2\theta = 43.5966$  (Fig. 24) shifts to  $2\theta = 50.9870$  (Fig. 25). Template based synthesis of single crystal copper nanowires have also been reported in literature [49, 97] with preferred growth direction along (111) plane.

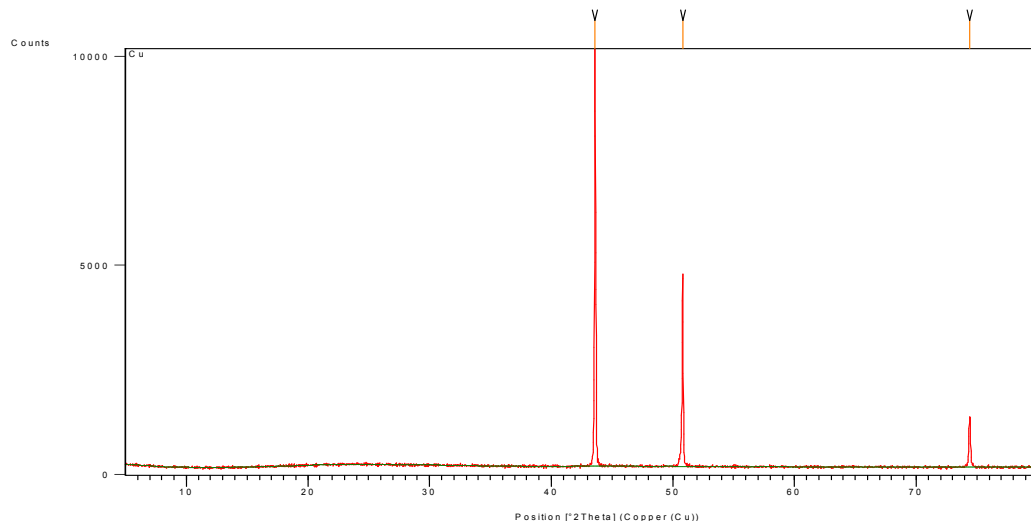
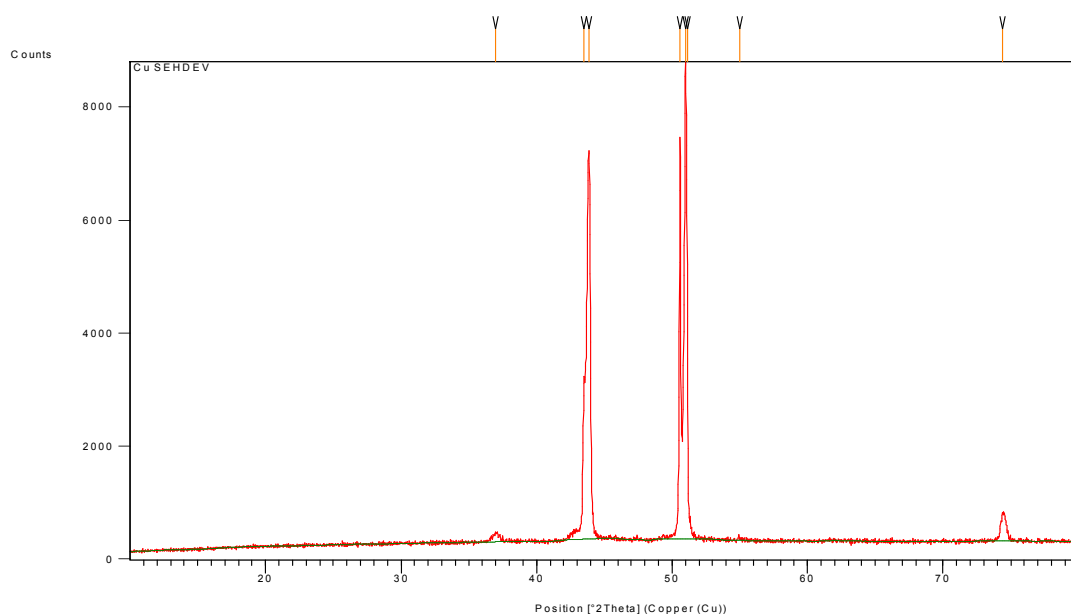
The average size  $D$  of the crystalline grains in the Cu nanowires is calculated using the Debye Scherrer's formula [140]:  $D = 0.9 \lambda / \beta \cos \theta$ , where  $\lambda=1.5406 \text{ \AA}$  is the wavelength of the X-ray radiation used,  $\beta$  is the full width at half maximum (FWHM) of the diffraction peak (0.1224), K, the shape factor is assumed to be 0.9 and  $\theta$  is the Bragg diffraction angle of the most prominent XRD peak. Substituting appropriate values in the formula, the crystallite size value of Cu nanowires comes out to be 1.22 nm. However, the value of crystallite size calculated for Cu foil is exact double, of the order of 2.44 nm.

**Table 1** XRD spectrum peaks data of copper film

Pos. [ $^{\circ}2\text{Th.}$ ]	FWHM [ $^{\circ}2\text{Th.}$ ]	d-spacing [ $\text{\AA}$ ]	Rel. Int. [%]	Area [cts* $^{\circ}2\text{Th.}$ ]
43.5966	0.0612	2.07438	100.00	847.65
50.8127	0.0816	1.79542	48.53	548.43
74.4331	0.1428	1.27358	11.94	236.07

**Table 2** XRD spectrum peaks data of polycrystalline copper nanowires

Pos. [°2Th.]	FWHM [°2Th.]	d-spacing [Å]	Rel. Int. [%]	Area [cts*°2Th.]
37.0062	0.3346	2.42724	2.29	76.37
43.4706	0.0669	2.08010	33.59	223.69
43.8561	0.2509	2.06270	93.99	2347.28
50.5881	0.0816	1.80286	74.62	819.15
50.9870	0.1224	1.78969	100.00	1646.70
51.1172	0.1224	1.78544	87.56	1441.89
54.9761	0.4080	1.66889	0.75	41.24
74.4238	0.4080	1.27372	5.90	324.08

**Fig. 24** XRD spectrum of copper film serving as a substrate (cathode)**Fig. 25** XRD spectrum of copper nanowires of 200 nm diameter

Energy dispersive X-ray analysis (EDAX) of Cu nanowires was carried out at FESEM facility of Central Scientific Instruments Organization (CSIO), Chandigarh to determine chemical composition of nanowires. The spectrum (Fig. 26) reveals 3 peaks of copper with 100% pure copper content and no traces of any impurity in Cu nanowires. It also establishes that multiple XRD peaks are not due to any impurity but due to polycrystalline nature of Cu nanowires.

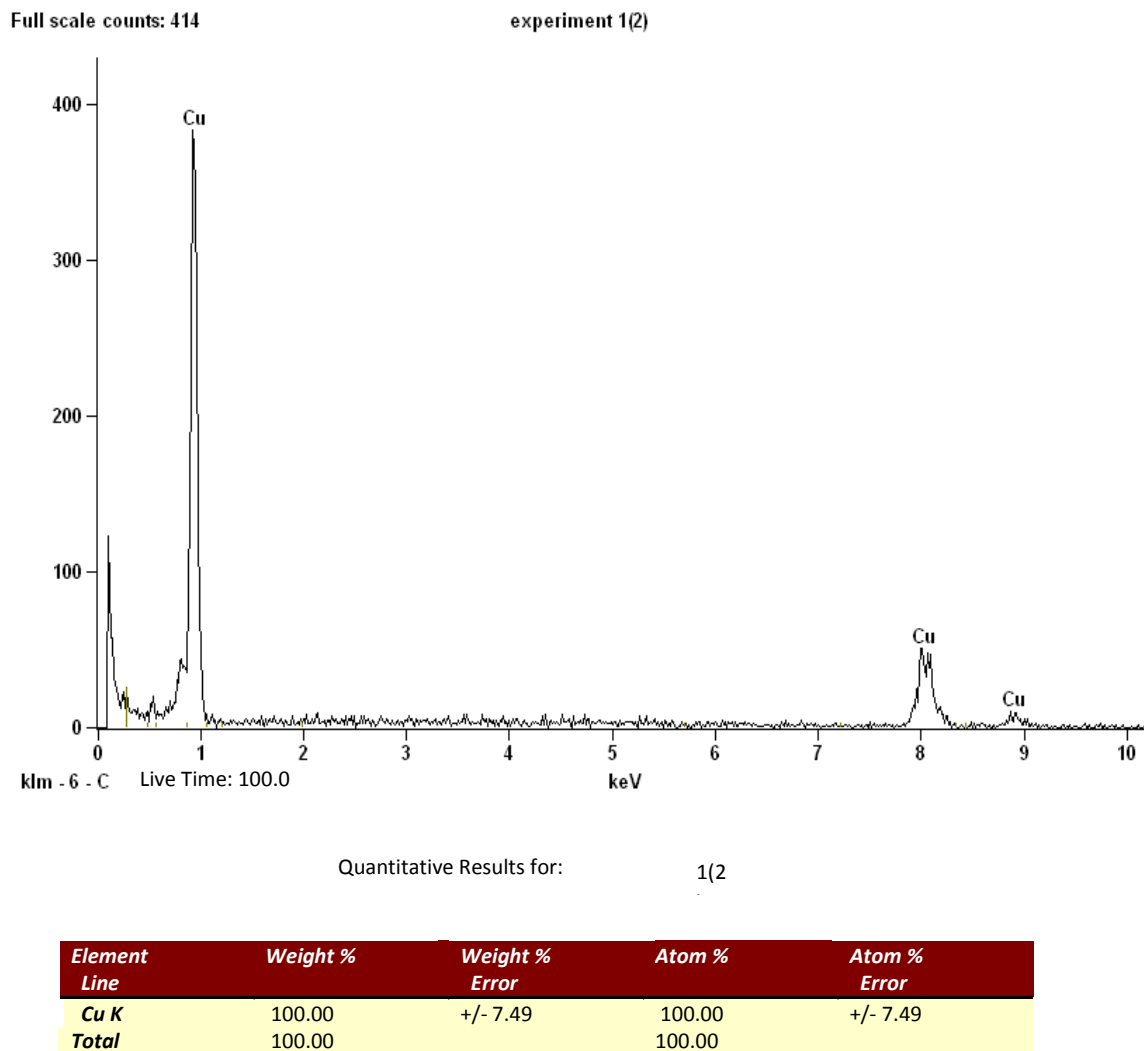


**Fig. 26** EDAX spectrum and elemental composition of Copper nanowires

**4.1.3 I-V Characteristics of Copper Nanowires.** I-V properties of aligned copper nanowires have been studied using a current-sensing AFM [95]. Electronic transport through nanocontacts has been an active area of research. The ultimate aim for nanowires is to find applications in the nanoelectronic devices. How can a copper nanowire produce a nonlinear I-V curve? The simplest possibility for observing such a phenomenon is generation of a tunnelling barrier at the wire-lead junction whose effect gradually collapses as a function of increasing bias voltage [141]. The nonlinear curves of Cu nanowire arrays may be caused by the existence of impurities (such as oxide) near the wire-lead contact region. Nonlinear phenomena of silver wire and gold wire have also been observed in air [141, 142]. It has been demonstrated that the nonlinear I-V characteristic is the basis of functional electronic devices [143].

I-V characteristics of copper nanowires were recorded in-situ, as grown in pores of anodic alumina template, using Dual Source Meter (Keithley Model 4200 SCS) with platinum probes for contacts. The combination of copper nanowires on alumina, an insulator, results in the formation of a strange device. I-V plot (Fig. 27) shows some interesting features of a resonating tunneling diode in the forward bias mode but nothing special in the reverse bias mode. The offset in I-V plot around zero

voltage may be due to slight non-ohmic characteristic of the contact, or due to quantum confinement behavior of electrons traversing through copper nanowires.

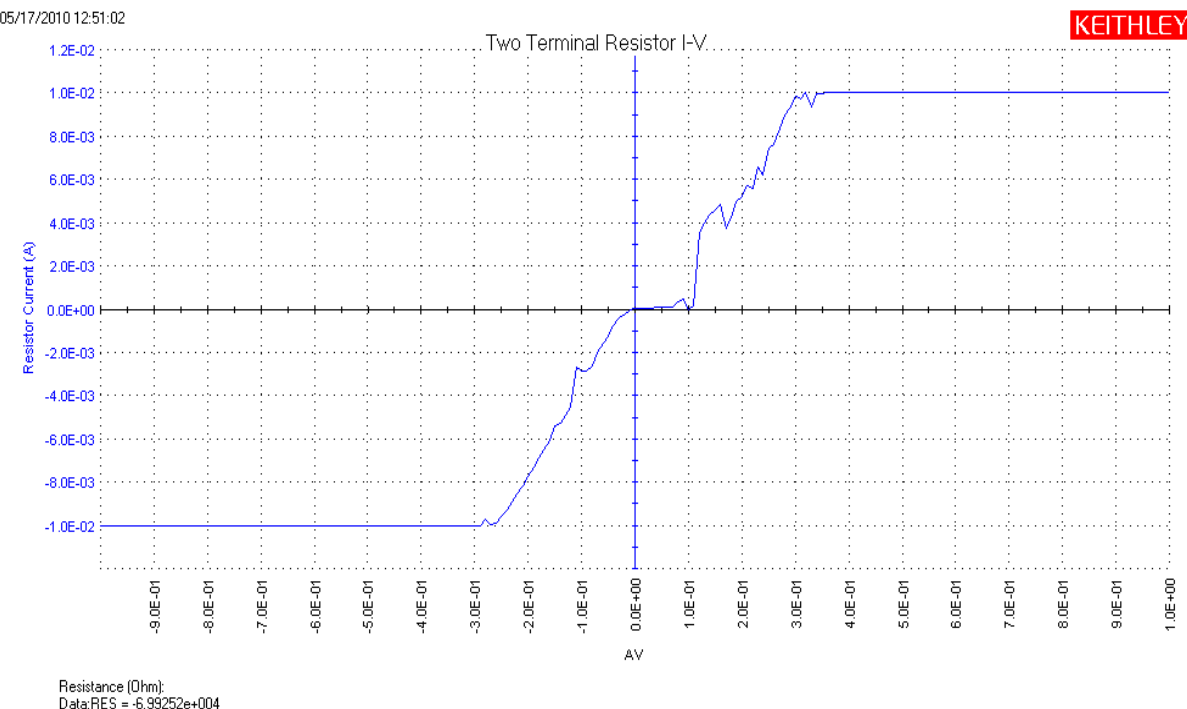


**Fig. 27** I-V characteristics of copper nanowires grown in-situ in anodic alumina template

## 4.2 Chartacterization of Semiconductor Nanowires

**4.2.1 Synthesis of CdS Nanowires.** CdS is one of the most important II–VI group semiconductors and has a band gap 2.42 eV at room temperature. CdS nanowires, in particular, have been extensively studied due to their potential applications in FETs, LEDs, photocatalysis and crossed Si-CdS nanowires recently used in nanoscale injection laser and in integrated photonics [12, 144–146]. Recently, CdS nanowires have been fabricated by *dc* and *ac* electrodeposition in non-aqueous solution containing CdCl<sub>2</sub> and elemental S, but high temperature and expensive organic reagent DMSO (dimethylsulfide) is necessary in order to dissolve elemental S in this method. Routkevitch et al. [56] reported that *ac* electrodeposition in an AAM template is a simple and efficient method to fabricate aligned CdS nanowires. However, a density of defects such as stacking faults and twinned segments have been observed in those nanowires. We preferred to use *dc* electrodeposition approach to obtain aligned and well distributed nanowire arrays, as well as uniform single crystal structure. The mechanism of CdS nanowires synthesis and chemical reactions involved has been given by Yang et al. [147].

CdS nanowires were fabricated by electrodeposition using commercially available AAM (anodisc 25, Whatmann, UK) having an average pore diameter of 200 nm, a nominal thickness of 60 µm and a pore density of 10<sup>9</sup> pores/cm<sup>2</sup>. A copper film was deposited by vacuum evaporation onto the back of the AAM template. Electrochemical cell (Fig. 11) was used for fabrication of CdS nanowires. A silver rod was used as an anode and the cathode consists of copper foil attached to copper coated AAM by an adhesive tape of good conductivity. The electrolyte solution consisted of 0.055M CdCl<sub>2</sub> and 0.19M elemental sulphur in dimethyl sulphoxide (DMSO). This solution prevents the corrosion of AAM during the deposition. The growth of CdS nanowires was carried out for 10 min. at a solution temperature of 80 °C with a *dc* potential of 2V applied between Ag anode and Cu cathode. The deposited samples were washed with hot DMSO to remove excess sulphur from the surface followed by rinsing in de-ionised water.

**4.2.2 SEM, HRTEM and EDAX Analysis.** Experimental details for preparation of samples are given by Virk [112]. Field Emission Scanning Electron Microscope (FESEM, Hitachi S-4300) was

used to record cross-sectional (Fig. 28a) and lateral views (Fig. 28b) of grown nanowires at an accelerating voltage of 15 kV using different magnifications. Figure 28(b) shows the majestic view of CdS nanowires grown in a cleavage or crack along the AAM which facilitates the electrodeposition process. High Resolution Transmission Electron Microscope (HRTEM, Hitachi H 7500) was used for investigation of CdS nanowire diameters and heterojunctions. For this purpose, nanowire arrays were removed from the template in ethanol and a few drops of this solution were loaded on carbon coated gold grids and inserted in HRTEM. Measurements were carried out in imaging mode at 80 kV under ultra high vacuum conditions as shown in figure 29 (a, b). CdS nanowires have non-uniform diameter as shown in Fig. 29 (a), and hetero-junctions as shown in Fig. 29 (b).

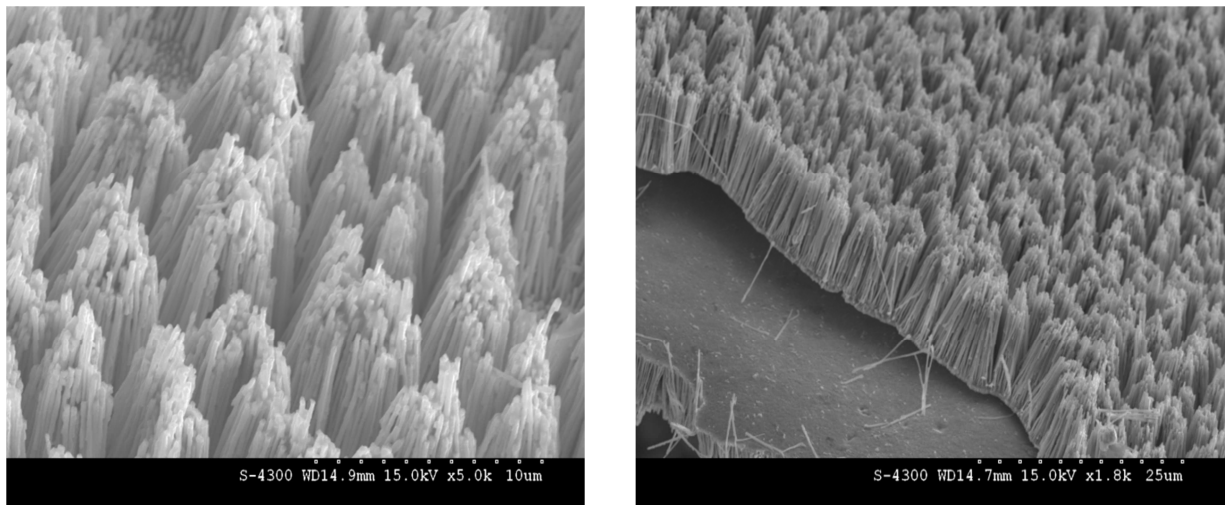


**Fig. 28** SEM micrograph showing (a) top cross-sectional and (b) lateral view of CdS nanowires

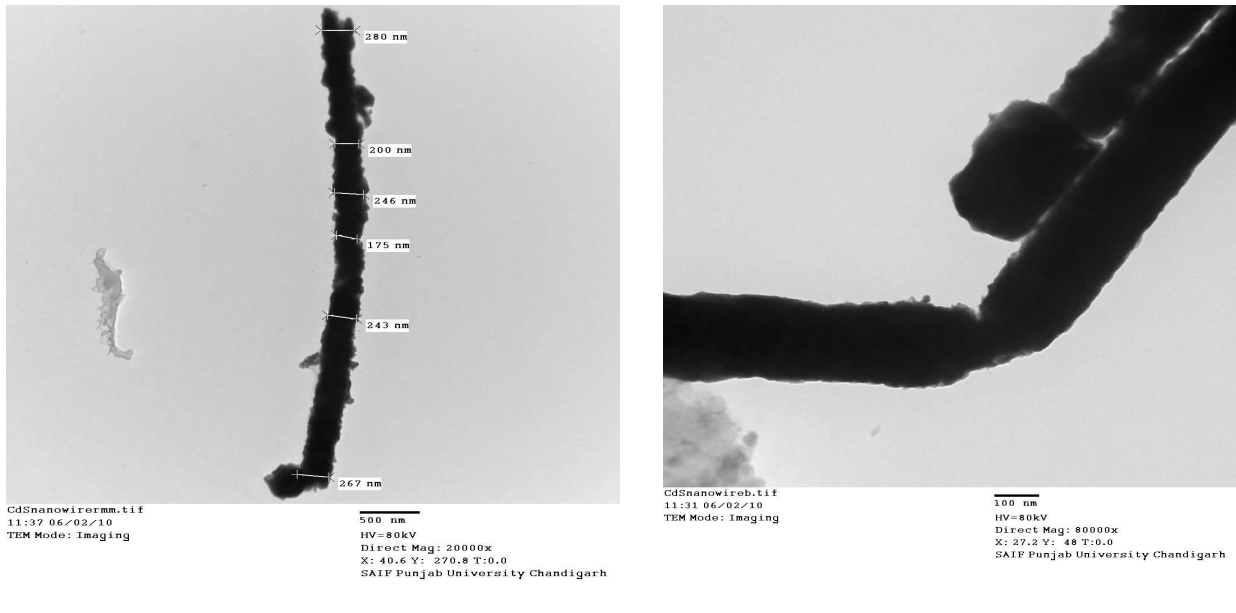


**Fig. 29** HRTEM images showing (a) CdS nanowire diameter variation, and (b) heterojunctions

For the quantitative compositional analysis, the chemical composition of nanowires was determined using energy dispersive X-ray analysis (EDAX) technique at FESEM facility of CSIO, Chandigarh. EDAX spectrum (Fig. 30) reveals prominent peaks due to Cu, Cd and S. There are also peaks

corresponding to elemental composition represented by Al, O and Cr. The Al peak is due to some residue of AAM which is not dissolved fully by NaOH treatment. The Cu peaks appear due to the effect of the substrate, which is copper film acting as the cathode.

Table 3 represents the elemental composition of CdS nanowires. The stoichiometry of CdS is almost 1:1 by weight % composition. The atomic % composition of all the elements is summarized in Table 1. Oxygen and Copper constitute almost 50% and 25%, respectively, of total composition. Impurity peak of chromium (Cr) is not reflected in elemental composition and can be ignored. Some other authors [147-149] have reported that the atomic composition of Cd and S in CdS nanowires is close to 1:1 stoichiometry using EDAX, as observed in our investigations. Sun Li et al. [149] have recently reported synthesis of sulphide nanowire arrays of CdS and ZnS through template-assisted electrodeposition. They observed phonon quantum confinement in nanowires using resonant Raman spectroscopy at room temperature.

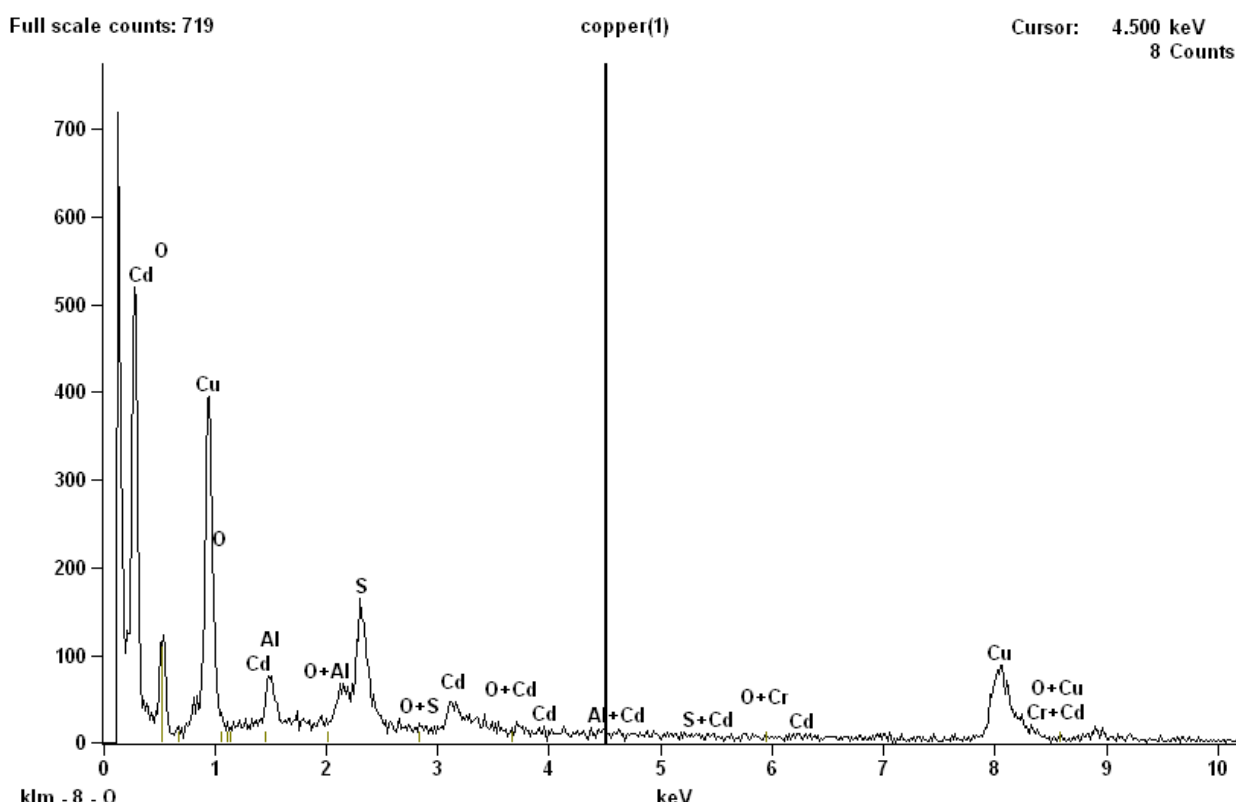


**Fig. 30** EDAX spectrum of CdS nanowires showing some prominent peaks of Cd, Cu, S, O, Al

**Table 3** Elemental composition of CdS nanowires

Element	Weight %	Weight %	Atom %	Atom %
Line	Error		Error	
<b>O K</b>	23.19	+/- 0.80	50.43	+/- 1.73
<b>Al K</b>	6.22	+/- 0.69	8.02	+/- 0.89
<b>S K</b>	11.06	+/- 0.53	12.00	+/- 0.58
<b>Cu K</b>	46.73	+/- 3.60	25.58	+/- 1.97
<b>Cd L</b>	12.80	+/- 1.94	3.96	+/- 0.60
<b>Total</b>	100.00		100.00	

#### 4.2.3 I-V Characteristics of CdS Nanowires

I-V characteristics of CdS nanowires exhibit some interesting features. A prominent feature of I-V plot (Fig. 31) is a number of peaks and valleys showing decrease in current with increase of voltage, resulting in negative differential resistance (NDR). This behavior is typical of a resonant tunneling diode (RTD) in which electrons can tunnel through some resonant states at certain energy levels. The presence of several NDR zones on the I-V plot is a definite proof of a RTD structure in CdS nanowires. HRTEM image (Fig. 29 b) shows formation of heterojunctions of CdS. In the literature, RTDs fabricated by InAs/InP III-V nanowire heterostructures have been reported [136]. It has been established that quantum size effects become pronounced as the size of the material approaches nanometer range [150].

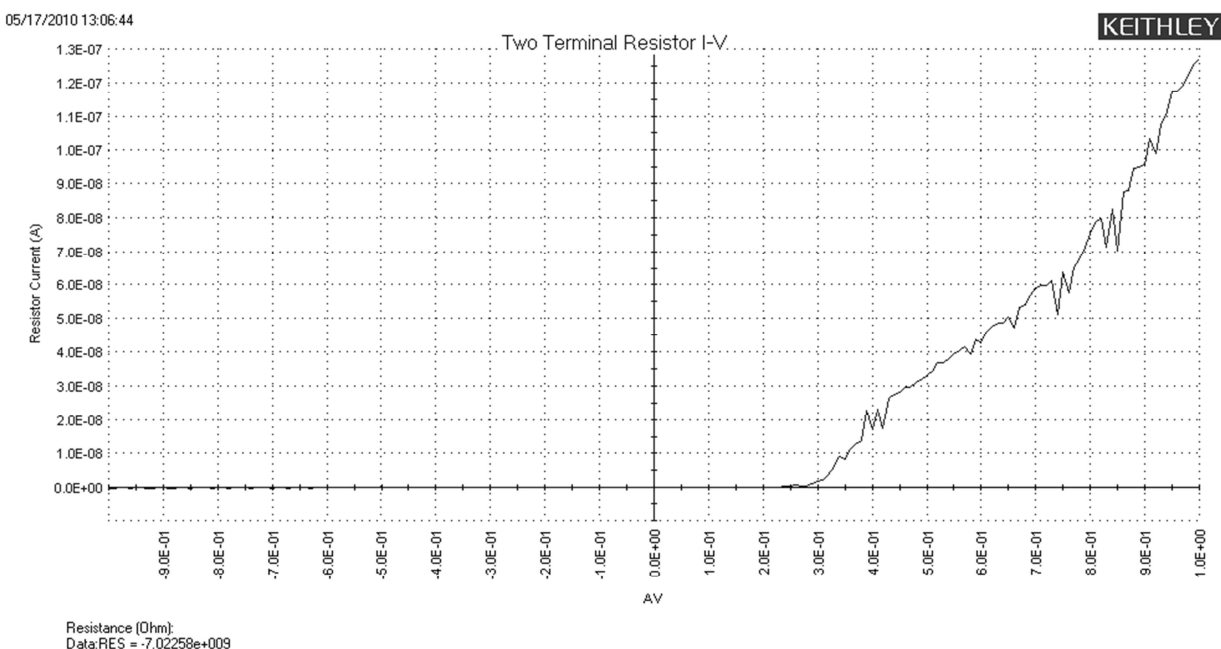


**Fig. 31** I-V plot of CdS nanowire diode arrays showing RTD characteristics prominently

#### 4.3 Characterization of Metal-Semiconductor Heterojunctions

**4.3.1 Synthesis of Cu-Se Nanowires.** Cu-Se nanowires were synthesized in an electrochemical cell as described in section 3.1. The electrolyte used had a composition of 200 gm/l CuSO<sub>4</sub>.5H<sub>2</sub>O + 25% of dilute H<sub>2</sub>SO<sub>4</sub> at room temperature, the inter-electrode distance was kept 0.5 cm and a potential difference of 2V was applied for 10 min using a *dc* source. When the anodic alumina template pores were approximately half-filled up with copper metal, the electrolyte was drained out and a second electrolyte having a composition of SeO<sub>2</sub> ( $8 \times 10^{-4}$  M) with 0.5 ml of 35% dilute H<sub>2</sub>SO<sub>4</sub> was introduced. A potential difference of 1V was applied for 15 min. at 60°C to electro-deposit Se semiconductor over Cu metal already deposited in pores. After the electrodeposition was over, the electrolyte was drained out and the cathode was rinsed with high purity water and ethanol. The filled template with copper backing was immersed in 1N NaOH for 1h to dissolve anodic alumina completely and to liberate the Cu-Se hetero-junctions in the shape of nanowires [133]. During the deposition process, we recorded the electrical current as a function of time. A typical chronoamperometric curve [39] was obtained.

**4.3.2 SEM, HRTEM and EDS Analysis.** The morphology of Cu-Se hetero-junctions has been revealed in SEM micrographs (Fig. 32). The dimensions of Cu-Se hetero-junctions are consistent with the pore dimensions of AAM. SEM images of fabricated hetero-junctions reveal a parallel alignment with approximately equal wire length. The SEM micrograph (Fig. 32b) reveals exuberant growth of Cu-Se nanowires in a cleavage or a crack which appeared during electrodeposition process in the template.

High Resolution Transmission Electron Microscope (HRTEM, Hitachi H 7500) was used for investigation of Cu-Se nanowire diameters and heterojunctions. For this purpose, nanowire arrays were removed from the template in ethanol and a few drops of this solution were loaded on carbon coated gold grids and inserted in HRTEM. TEM measurements show irregular shape of nanowires with diameter variation from 228 nm to 395 nm (Fig. 33 a). Figure 33 (b) shows the morphology of a hetero-junction of Cu-Se nanowire.

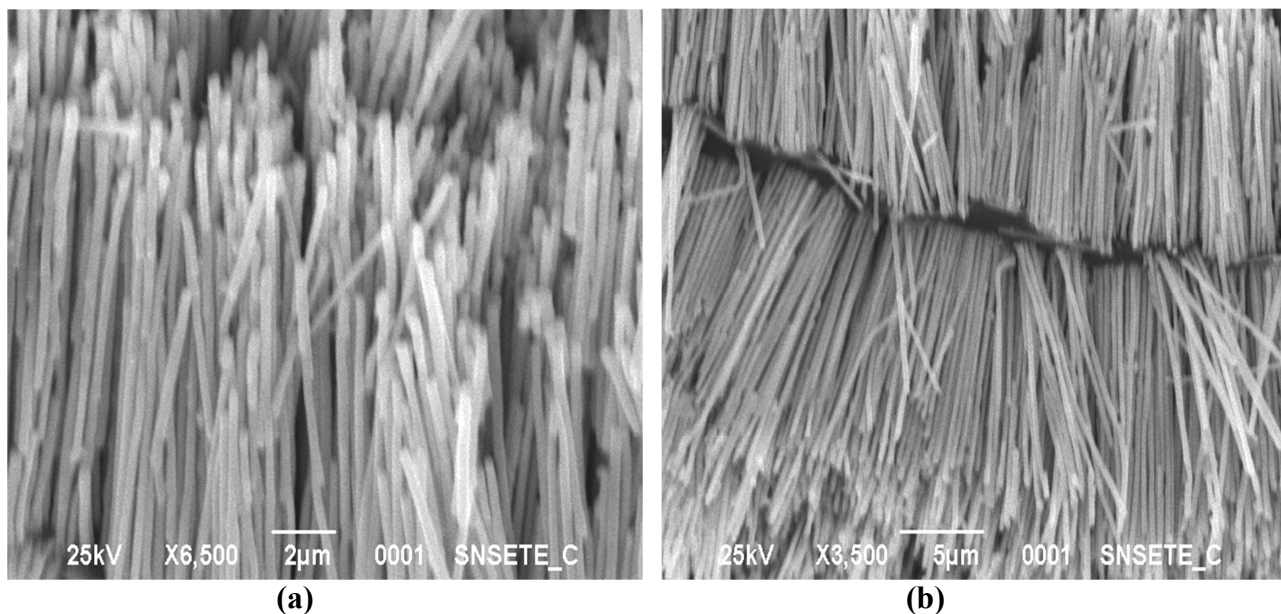


**Fig. 32** SEM micrographs showing (a) morphology of Cu-Se heterojunctions, and (b) Cu-Se nanowires grown in a cleavage or a crack in AAM

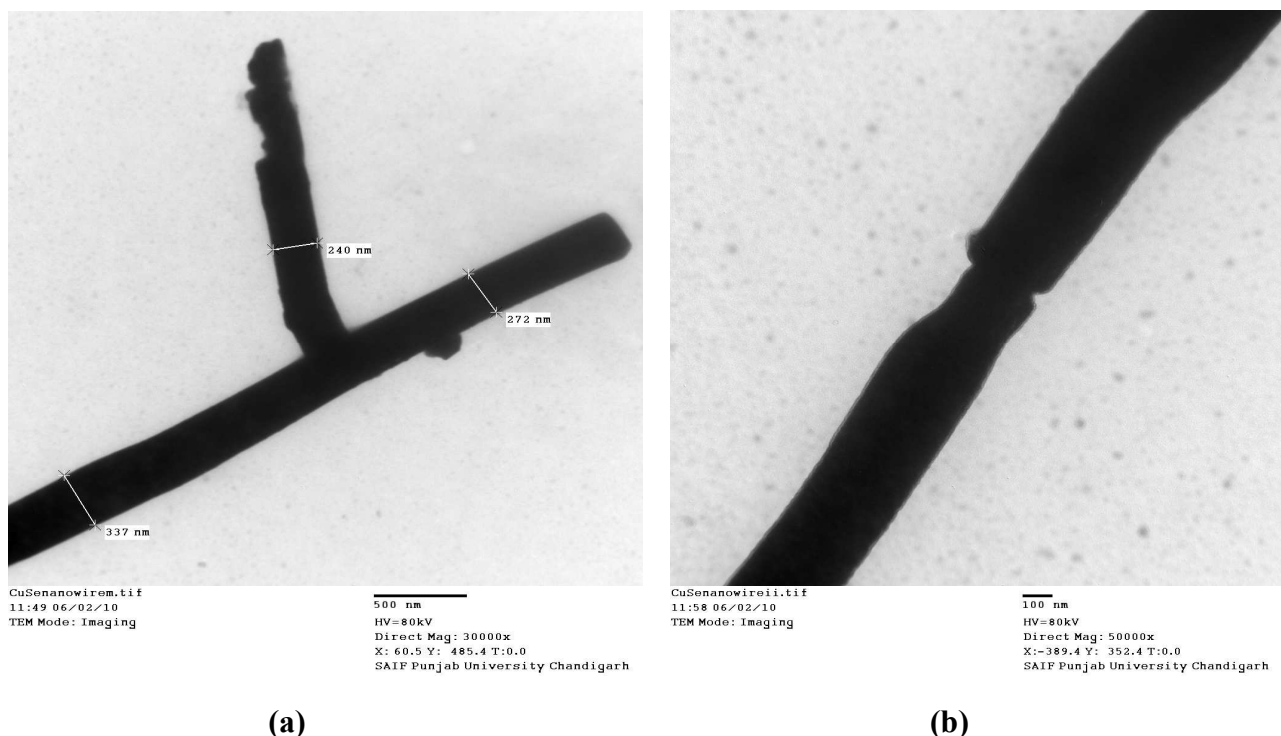


**Fig. 33** HRTEM images showing (a) branched Cu-Se nanowire with diameter variation, and (b) showing a Cu-Se junction in the nanowire

Chemical composition of liberated Cu-Se hetero-junctions is determined using Energy Dispersive X-ray Spectroscopy (EDS) facility at PAU, Ludhiana. EDS spectrum (Fig. 34) reveals that Cu-Se hetero-structures are composed of mainly Cu and Se metals. There are also peaks corresponding to

elemental composition represented by C, N and O. The prominent peaks are representative of Cu and Se in Cu-Se heterostructures. Table 4 represents the elemental composition of Cu-Se heterojunctions. The stoichiometry of Cu-Se is almost 1:1 by weight % composition. The atomic % composition of all the elements is summarized in Table 4. Carbon atoms have highest atomic % composition which is quite unusual. It may be concluded that template synthesis using AAM is an efficient tool for fabrication of Cu-Se heterojunctions of pre-determined morphology and stoichiometry.

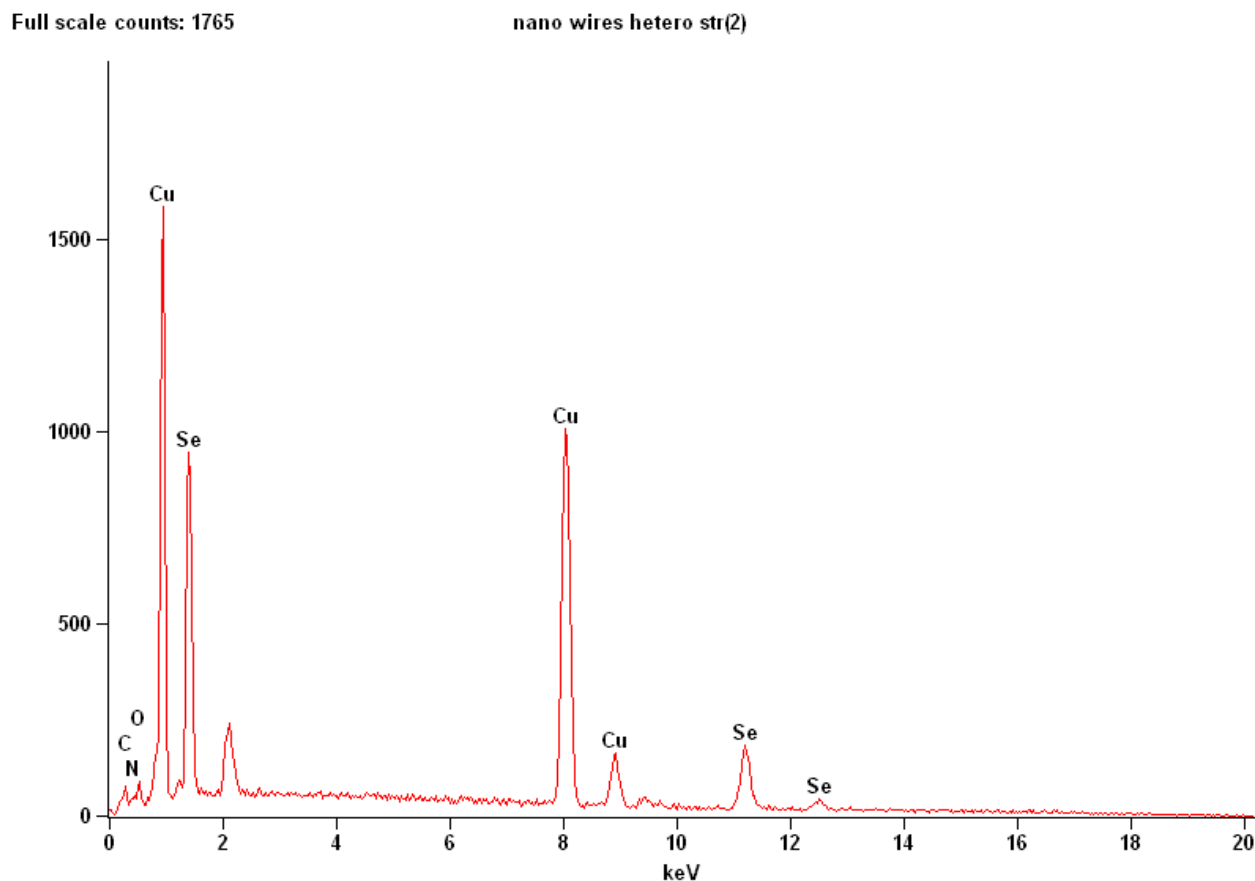


**Fig. 34** EDS spectrum showing elemental composition of Cu-Se heterostructures

**Table 4** Elemental composition of Cu-Se heterojunctions

Element	Net Counts	Net Counts Error	Weight %	Atom %
C	571	+/- 56	13.09	42.57
N	205	+/- 55	2.75	7.66
O	435	+/- 76	1.46	3.55
Cu	17511	+/- 266	44.31	27.23
Se	3292	+/- 187	38.39	18.99
<b>Total</b>			100.00	100.00

**4.3.3 I-V characteristics of Cu-Se Heterostructures.** I-V characteristics of Cu-Se/CdSe heterojunctions have been studied by some groups in India [130-132] to determine resonant tunneling diode behavior of fabricated devices/junctions. We failed to observe such behavior during our investigations. A prominent feature of I-V plot (Fig. 35) is a smooth curve showing increase of current with increase of voltage, in both forward and reverse bias modes. We can attribute this behavior to Se semiconductor acting as a p-n junction diode but not to a resonant tunneling diode (RTD).

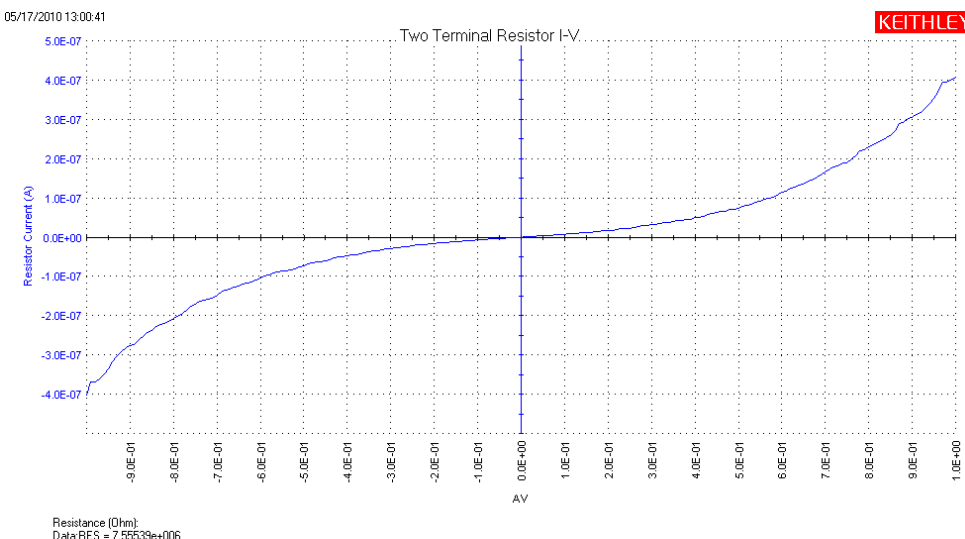


**Fig. 35** I-V Plot of Cu-Se hetero-junctions showing p-n junction diode behavior

## 5. Bulk Production of Copper Nanowires

Bulk production of Copper Nanowires (CuNWs) has been achieved recently by seed growth technique by Rathmell et al. [151]. The development of a high-performance transparent conductor that is also inexpensive, flexible, and can be deposited at low temperatures would remove a significant barrier to the development of low-cost flexible displays, lighting, and solar cells. Here we report the gram-scale synthesis of copper nanowires in aqueous solution, and their assembly into flexible films that transmit nearly 15% more light than films of carbon nanotubes. We further show that copper nanowires exhibit a unique growth mechanism in that they sprout and grow from spherical copper seeds.

CuNWs were synthesized by reducing  $\text{Cu}(\text{NO}_3)_2$  with hydrazine in an aqueous solution containing NaOH and ethylenediamine (EDA), following the approach developed by Chang et al. [152]. To demonstrate its potential for large-scale production, the reaction was scaled by 200 times (from 0.006 to 1.2 g of CuNWs). For the scale up reaction (Fig. 36), NaOH (2000 ml, 15M),  $\text{Cu}(\text{NO}_3)_2$  (100 ml, 0.2M), EDA (30 ml), and hydrazine (2.5 ml, 35 wt%) were added to a reaction flask and heated at 80 °C for 60 minutes. The solution went from a royal blue (Fig. 36a), indicative of  $\text{Cu}^{2+}$  ions, to a reddish brown color indicative of CuNW formation (Figure 36b) after 20 minutes. The nanowires are  $90 \pm 10$  nm in diameter and  $10 \pm 3$   $\mu\text{m}$  in length (Fig. 36c). After the reaction, the CuNWs were washed with a 3 wt % aqueous solution of hydrazine, and stored in the same hydrazine solution at room temperature under an argon atmosphere to minimize oxidation [152].

The CuNWs grew via atomic addition to {110} planes, which have the highest surface energy among the low-index facets of copper and all other FCC metals [153 –155]. During the reaction, the CuNWs form a cake that floats on the top of the solution due to the bubbles of  $\text{N}_2$  generated by decomposition of hydrazine. This aggregate of wires must be dispersed before the wires are used to make a transparent electrode. It has been shown that CuNWs sprout and grow from spherical seeds, with the concentration of EDA being a critical parameter for their anisotropic growth. Films of CuNWs transmit nearly 15% more light than films of CNTs, but 25% less than ITO films with the same sheet resistance. The experimental data indicate that the transmittance of CuNW films is not limited by the optical properties of copper, but by the aggregation. If aggregation of CuNWs can be eliminated, the properties of films of CuNWs should be on par with films of AgNWs, and very close to those of ITO. With their low cost (copper is 1/100th the cost of indium), flexibility, and the fact they are grown in and deposited from aqueous solution, CuNWs could revolutionize the development and production of low-cost flexible displays [156], light emitting diodes [157 ], and thin film solar cells [158].

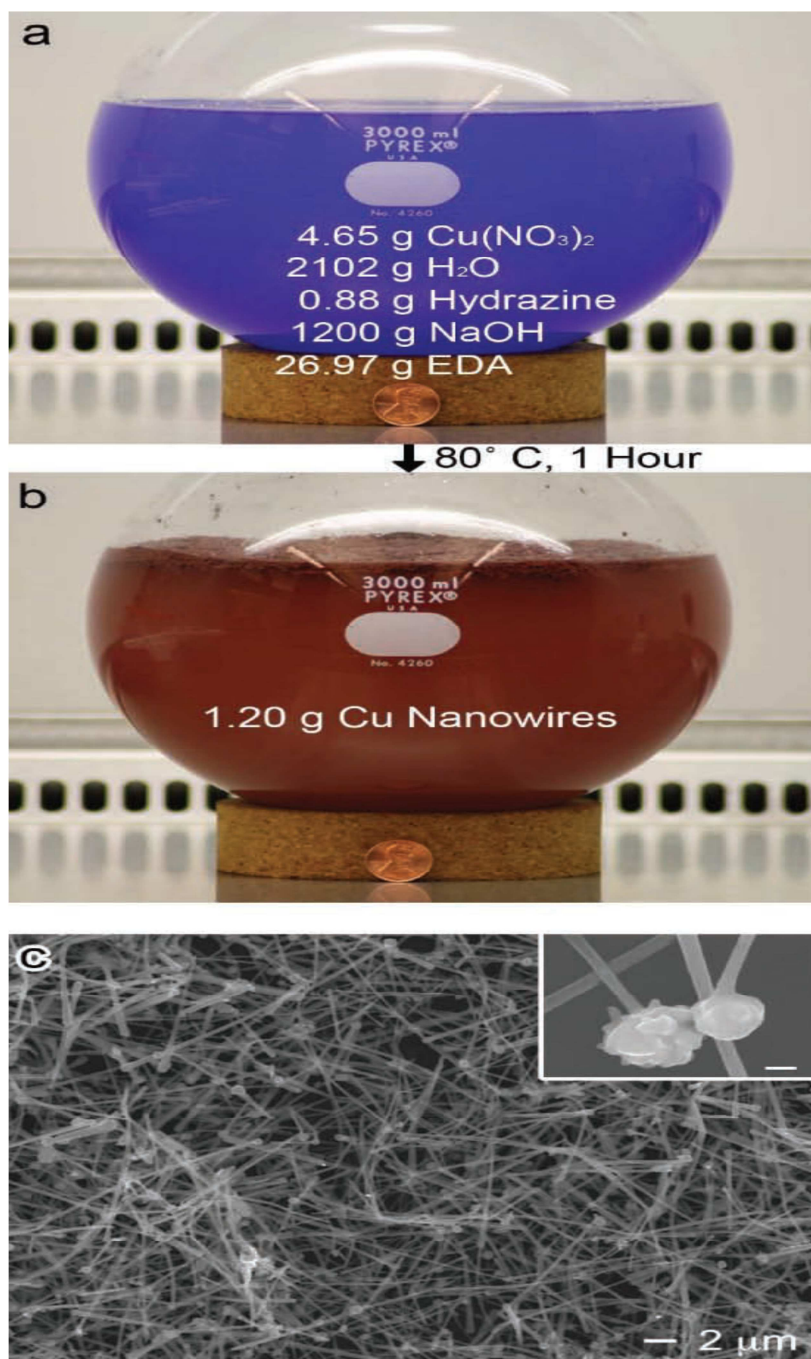


**Fig. 36** The image of reaction flask (a) before the synthesis, (b) after the growth of CuNWs at 80 °C for 1 hr. (c) SEM image of CuNWs product. The inset shows CuNWs with spherical copper particles attached at one end (scale bar = 200 nm) [adopted from ref. 149].

## 6. Summary

A detailed review for the synthesis of metallic and semiconductor nanowires has been reported in this review paper. Template-assisted synthesis of nanowires has caught the fancy of the present author and the research work carried out in his laboratory forms the core of this review. The preparation of anodic alumina and polymer templates has been discussed in detail. A comparison of both the techniques has been made. Electrodeposition of metallic and semiconductor nanowires synthesis has been carried out in a cell fabricated in author's laboratory. A wide variety of templates are available in the market but most of the laboratories use either template-assisted synthesis or Vapour-Liquid-Solid (VLS) method for nanowire synthesis. Interestingly, silicon and germanium nanowires grown by the VLS method consist of a crystalline core coated by a

relatively thick amorphous oxide layer. A variety of semiconductor nanowires have been fabricated using VLS and electrochemical deposition techniques from materials including ZnO, ZnS, GaN, CdS, CdSe, CdO, ZnSe, InP, GaAs and Se.

Characterization of metal and semiconductor nanowires has been accomplished using scanning electron microscope (SEM), field emission scanning electron microscope (FESEM), high resolution transmission microscope (HRTEM), X-ray diffraction (XRD), and energy dispersive X-ray analysis (EDAX). XRD revealed mono- and poly-crystalline nature of copper nanowires and chemical composition by EDAX. TEM images of CdS nanowires and Cu-Se heterojunctions reveal variation of diameter and nature of heterojunctions. I-V characteristics of copper and semiconductor CdS nanowires were recorded in-situ, as grown in pores of anodic alumina template, using Dual Source Meter (Keithley Model 4200 SCS) with platinum probes for contacts. Resonating tunneling diode (RTD) characteristics of fabricated CdS nanowires have been investigated. Bulk production of copper nanowires by seed growth technique has been discussed.

### Acknowledgements

Research work reported in this review paper has been carried out in Centre for Nanotechnology of DAV Institute of Engineering and Technology (DAVIET), Jallandhar City, Punjab (India). Financial support of DAV Colleges Managing Committee, New Delhi is acknowledged. Author wishes to thank his team of workers, namely, Kamal Kishore, Vishal Balouria, Gurmit Singh Lotey, Sehdev Chauhan, Vinay Bhat, Sanjit Amrita and Sanjeev Mahajan for help in the experimental work. Ranjit Singh Gehrotra helped the author in fabrication of the Electrochemical cell. Special thanks are due to several scientists who provided generous support by supplying their published review papers on this topic, viz., M.S. Dresselhaus, C.M. Leiber, C.Z. Cao and N. Wang, among many others. I am indebted to my family members in India and abroad for their moral support for undertaking this strenuous task.

### References

- [1] Ratner and D. Ratner, Nanotechnology: A gentle introduction to the next big idea, Pearson Education Publication, London, 2003.
- [2] G. Z. Cao, Nanostructures and Nanomaterials, Imperial College Press, London, 2004.
- [3] S. Bandyopadhyay and H.S. Nalwa (Eds.), Quantum Dots and Nanowires, American Scientific Publishers, USA, 2003.
- [4] W.M. Tolles and B.B. Rath, Nanomaterials: Synthesis, Processing and Applications (Eds. A.S. Adelstein and R.C. Cammarata), Inst. of Physics, 1996, pp. 545-553; Nanotechnology, a stimulus for innovation, Curr. Sci. 85 (12) (2003) 1746-1759.
- [5] J. Sarkar, G.G. Khan and A. Basumallick, Nanowires: properties, applications and synthesis via porous anodic aluminium oxide template, Bull. Mater. Sci. 30(3) (2007) 271-290.
- [6] H. Sun Shin, J. Y. Song and J. Yu, Template-assisted electrochemical synthesis of cuprous oxide nanowires, Materials Letters 63 (2009) 397-399.
- [7] R. Ingunta, S. Piazza and C. Sunseri, Novel procedure for the template synthesis of metal nanostructures, Electrochim. Commun. 10 (2008) 506-509.
- [8] M. S. Dresselhaus, Y. M. Lin, O. Rabin, M. R. Black, G. Dresselhaus, Nanowires, A review listed on: [mgm.mit.edu/group/x986.pdf](http://mgm.mit.edu/group/x986.pdf), Jan. 2, 2003.
- [9] H. S. Virk, Fabrication and Characterization of Copper Nanowires, in: Abbass Hashim (Ed.), Nanowires - Implementations and Applications, InTech Open Publishers, Rijeka, 2011, pp. 455-470, <http://www.intechopen.com/articles/show>

- [10] Y. Cui, and C.M. Lieber, Functional nanoscale electronic devices assembled using silicon nanowire building blocks, *Science* 291 (2001), 851–853.
- [11] X. Duan, Y. Huang, Y. Cui, J. Wang and C.M. Lieber, Indium phosphide nanowires as building blocks for nanoscale electronic and optoelectronic devices, *Nature* 409 (2001) 66–69.
- [12] R. Aggarwal and C.M. Leiber, Semiconductor nanowires: optics and optoelectronics, *Appl. Phys. A* 85 (2006) 209-215.
- [13] M. H. Huang, S. Mao, H. Feick, H. Yan, Y. Wu, H. Kind, E. Weber, R. Russo, and P. Yang, Room-temperature ultraviolet nanowire nanolasers, *Science* 292 (2001) 1897–1899.
- [14] Y. Cui, Q. Wei, H. Park, and C.M. Lieber, Nanowire nanosensors for highly sensitive and selective detection of biological and chemical species, *Science* 293 (2001) 1289–1292.
- [15] M. Law, L.E. Greene, J.C. Johnson, R. Saykally and P. Yang, Nanowire dye-sensitized solar cells, *Nat. Mater.* 4(6) (2005) 455–459.
- [16] Y. Li, F. Qian, J. Xiang and C.M. Lieber, Nanowire electronic and optoelectronic devices, *Mater. Today* 9(10) (2006) 18–27.
- [17] C. Thelander, P. Agarwal, S. Brongersman, J. Eymery, L.F. Feiner, A. Forchel, M. Scheffler, W. Riess, B.J. Ohlsson, U. Gösele and L. Samuelson, Nanowire-based one-dimensional electronics, *Mater. Today* 9(10) (2006) 28–35.
- [18] K. Ramanathan, M.A. Bangar, M. Yun, W. Chen, N.V. Myung and A. Mulchandani, Bioaffinity sensing using biologically functionalized conducting-polymer nanowire, *J. Am. Chem. Soc.* 127(2) (2005) 496–497.
- [19] N. Wang, Y. Cai and R.Q. Zhang, Growth of nanowires, *Mater. Sci. Eng. R-Rep.* 60 (2008) 1–51.
- [20] G. Cao and D. Liu, Template based synthesis of nanorod, nanowire, and nanotube arrays, *Adv. In Colloid & Interface Sci.* 136 (2008) 45-64.
- [21] S. Amrita Kaur, Preparation and Applications of Ion Track Filters, Ph. D. Thesis submitted to Guru Nanak Dev University, Amritsar, 1998 (Unpublished).
- [22] S. Amrita Kaur, H.S. Virk and S.K. Chkravarti, Application of ion track filters: Our experience, Proc. 3rd Int. Conf. on Material Science applications of Ion Beam Techniques held at Seeheim, Germany, 9-12 September, 1996. Materials Science Forum, 248-249 (1997) 467-470.
- [23] H.S. Virk and S. Amrita Kaur, Ion Track Filters: Properties, Development and Applications, *Curr. Sci.* 75 (8) (1998) 765-770.
- [24] H.S. Virk, S. Amrita Kaur and G.S. Randhawa, Effects on insulators of swift-heavy-ions radiation: Ion track technology, *J. of Phys. D: App. Phys.* 31 (1998) 3139-3145.
- [25] G.A. Ozin, Nanochemistry: synthesis in diminishing dimensions, *Adv. Mater.* 4 (1992) 612-649.
- [26] R.J. Tonucci, B.J. Justus, A.J. Campillo and C.E. Ford, Nanochannel array glass, *Science* 258 (1992) 783-785.
- [27] J.Y. Ying, Nanoporous Systems and Templates: The Unique Self-Assembly and Synthesis of Nanostructures, *Science Spectra* 18 (1999) 56-63.
- [28] J.W. Diggle, T.C. Downie and C.W. Goulding, Anodic oxide films on aluminum. *Chem. Rev.* 69 (1969) 365-405.
- [29] J.P. O'Sullivan and G.C. Wood, The morphology and mechanism of formation of porous anodic films on aluminum. *Proc. Roy. Soc. London A* 317 (1970) 511-543.

- [30] A.P. Li, F. Muller, A. Birner, K. Neilsch and U. Gosele, Hexagonal pore arrays with a 50-420 nm inter-pore distance formed by self-organization in anodic alumina. *J. Appl. Phys.* 84 (1998) 6023-6026.
- [31] O. Jessenky, F. Muller and U. Gossele, Self-organized formation of hexagonal pore arrays in anodic alumina, *Appl. Phys. Lett.* 72 (1998) 1173-1175.
- [32] D.A. Mawiawi, N. Coombs and M. Moskovits, Magnetic-properties of Fe deposited into anodic aluminum-oxide pores as a function of particle-size, *J. Appl. Phys.* 70 (1991) 4421-4425.
- [33] Z. Zhang, D. Gekhtman, M.S. Dresselhaus and J.Y. Ying, Processing and characterization of single-crystalline ultrafine bismuth nanowires. *Chem. Mater.* 11 (1999) 1659-1665.
- [34] F. Li, L. Zhang and R.M. Metzger, On the growth of highly ordered pores in anodized aluminum oxide, *Chem. Mater.* 10 (1998) 2470-2480.
- [35] V.D.R. Caffarena, J.L. Capataneo, R.A. Simao and A.P. Guimaraes, Preparation of electrodeposited Cobalt nanowires, *Mater. Res.* 9(2) (2006) 205-208.
- [36] E. Ferain and R. Legras, Track-etched membrane - dynamics of pore formation, *Nucl. Instrum. Methods B* 84 (1993) 331-336.
- [37] M.E. Toimil Molares, V. Buschmann, D. Dobrev, R. Neumann, R. Scholz, I.U. Schuchert and J. Vetter, Single-crystalline copper nanowires produced by electrochemical deposition in polymeric ion track membranes, *Adv. Mater.* 13 (2001) 62-65.
- [38] C.R. Martin, Nanomaterials: A membrane-based synthetic approach, *Science* 266 (1994) 1961-1966.
- [39] M.E. Toimil Molares, J. Brotz, V. Buschmann, D. Dobrev, R. Neumann, R. Scholz, I.U. Schuchert, Trautmann and J. Vetter, Etched heavy ion tracks in polycarbonate as template for copper nanowires, *Nucl. Instrum. & Meth. Phys. Res. B* 185 (2001) 192-197.
- [40] H.S. Virk, Heavy ion tracks route to nanotechnology, *Adv. Mater. Res.* 67 (2009) 115-120.
- [41] L. Sun, P. Searson and C.L. Chien, Electrochemical deposition of nickel nanowire arrays in single- crystal mica films, *Appl. Phys. Lett.* 74 (1999) 2803-2805.
- [42] C.A. Huber and T.E. Huber, A novel microstructure: Semiconductor-impregnated porous Vycor glass. *J. Appl. Phys.* 64 (1988) 6588-6590.
- [43] J.S. Beck, J.C. Vartuli, W.J. Roth, M.E. Leonowicz, C.T. Kresge, K.D. Schmitt, C.T. W. Chu, D.H. Olson, E.W. Sheppard, S.B. McCullen, J.B. Higgins and J.L. Schlenker, A new family of mesoporous molecular sieves prepared with liquid crystal templates. *J. Am. Chem. Soc.*, 114 (1992) 10834-10843.
- [44] C.G. Wu and T. Bein, Conducting polyaniline filaments in a mesoporous channel host, *Science* 264 (1994) 1757-1759.
- [45] E. Braun, Y. Eichen, U. Sivan and G. Ben-Yoseph, DNA-templated assembly and electrode attachment of a conducting silver wire, *Nature* 391 (1998) 775-778.
- [46] T. Thurn-Albrecht, J. Schotter, G.A. Kastle, N. Emley, T. Shibauchi, L. Krusin-Elbaum, K. Guarini, C.T. Black, M.T. Tuominen and T.P. Russell, Ultrahigh-density nanowire arrays grown in self-assembled diblock copolymer templates, *Science* 290 (2000) 2126-2129.
- [47] K. Liu, C.L. Chien, P.C. Searson and Y.Z. Kui, Structural and magneto-transport properties of electrodeposited bismuth nanowires. *Appl. Phys. Lett.* 73 (1998) 1436-1438; K. Liu, C. Chien and P.C. Searson, Finite-size effects in bismuth nanowires, *Phys. Rev. B* 58 (1998) R14681-R14684.

- [48] R. Ferre, K. Ounadjela, J.M. George, L. Piraux and S. Dubois, Magnetization processes in nickel and cobalt electrodeposited nanowires. *Phys. Rev. B* 56 (1997) 14066-14075.
- [49] T. Mingliang, J. Wang, J. Kurtz, T.E. Mallouk and M.H.W. Chan: Electrochemical Growth of Single-Crystal Metal Nanowires via a Two-Dimensional Nucleation and Growth Mechanism, *Nano Letters* 3 (2003) 919-923.
- [50] H. Zeng, M. Zheng, R. Skomski, D.J. Sellmyer, Y. Liu, L. Menon and S. Bandyopadhyay, Magnetic properties of self-assembled Co nanowires of varying length and diameter, *J. Appl. Phys.* 87 (2000) 4718-4720.
- [51] Y. Peng, H.L. Zhang, S.L. Pan and H.L. Li, Magnetic properties and magnetization reversal of  $\alpha$ -Fe nanowires deposited in alumina film, *J. Appl. Phys.* 87 (2000) 7405-7409.
- [52] M. Motoyama, Y. Fakunaka, T. Sakka, Y. Ogata and S. Kikuchi: Electrochemical processing of Cu and Ni nanowire arrays, *J. Electroanal. Chem.* 584 (2005), 84-91.
- [53] G. Sauer, G. Brehm, S. Schneider, K. Nielsch, R.B. Wehrspohn, J. Choi, H. Hofmeister and U. Gosele, Highly ordered monocrystalline silver nanowire arrays, *J. Appl. Phys.* 91 (2002) 3243-3247.
- [54] G.L. Hornyak, C.J. Patrissi and C.M. Martin, Fabrication, characterization, and optical properties of gold nanoparticle/porous alumina composites: the nonscattering Maxwell-Garnett limit, *J. Phys. Chem. B* 101 (1997) 1548-1555.
- [55] G.Yi and W.Schwarzacher, Single crystal superconductor nanowires by electrodeposition, *Appl. Phys. Lett.* 74 (1999) 1746-1748.
- [56] D. Routkevitch, T. Bigioni, M. Moskovits and J.M. Xu, Electrochemical fabrication of CdS nanowire arrays in porous anodic aluminum oxide templates, *J. Phys. Chem.*, 100 (1996) 14073-14047.
- [57] Blondel, J.P. Meier, B. Doudin and J.P. Ansermet, Giant magnetoresistance of nanowires of multilayers, *Appl. Phys. Lett.* 65 (1994) 3019-3021.
- [58] L. Piraux, I.M. George, J.F. Despres, C. Leroy, E. Ferain, R. Legras, K. Ounadjela and A. Fertt, Giant magnetoresistance in magnetic multilayered nanowires, *Appl. Phys. Lett.* 65 (1994) 2484-2486.
- [59] D. Almawlawi, C.Z. Liu and M. Moskovits, Nanowires formed in anodic oxide nano-templates, *J.of Mater. Res.* 9 (1994) 1014-1018.
- [60] M.S. Sander, A.L. Prieto, R. Gronsky, T. Sands and A.M. Stacy, Fabrication of high-density, high aspect ratio large-area bismuth telluride nanowire arrays by electrodeposition into porous anodic alumina templates, *Adv. Mater.* 14 (2002) 665-667.
- [61] D.S. Xu, D.P. Chen, Y.J. Xu, X.S. Shi, G.L. Guo, L.L. Gui and Y.Q. Tang, Preparation of II-VI group semiconductor nanowire arrays by dc electrochemical deposition in porous aluminum oxide templates, *Pure Appl. Chem.* 72 (2000) 127-135.
- [62] D. Xu, Y. Xu, D. Chen, G. Guo, L. Gui and Y. Tang, Preparation of CdS single-crystal nanowires by electrochemically induced deposition, *Adv. Mater.*, 12 (2000) 520-522.
- [63] M. Lai and D.J. Riley, Templated electrosynthesis of nanomaterials and porous structures, *J. Colloid and Interface Sci.* 323 (2008) 203-212.
- [64] Bogomolov, Injection under high pressure of molten metals into crystalline materials containing regular cavities, *Sov. Phys. Solid State* 13 (1971) 815-818.
- [65] J.Y. Ying, Z. Zhang, L. Zhang and M.S. Dresselhaus, US Patent 20016231744 (2001).
- [66] R.M. Penner, M.P. Zach and F. Favier, US Patent 20056843902 (2005)

- [67] M.P. Zach, K.H. Ng, J.C. Hemminger and R.M. Penner, Synthesis of molybdenum nanowires with millimeter-scale lengths using electrochemical step edge decoration, *Chem. Mater.* 14 (2002) 3206.
- [68] M.P. Zach, K.H. Ng and R.M. Penner, Molybdenum nanowires by electrodeposition, *Science* 290 (2000) 2120.
- [69] R.S. Wagner and W.C. Ellis, Vapor-liquid-solid mechanism of single crystal growth, *Appl. Phys. Lett.* 4 (1964) 89-91.
- [70] Y. Wu and P. Yang, Direct observation of vapor-liquid-solid nanowire growth, *J. Am. Chem. Soc.* 123 (2001) 3165-3166.
- [71] Y. Cui, L.J. Lauhon, M.S. Gudiksen, J. Wang and C.M. Lieber, Diameter-controlled synthesis of single crystal silicon nanowires, *Appl. Phys. Lett.* 78 (2001) 2214-2216.
- [72] Y. Wu and P. Yang, Germanium nanowire growth via simple vapor transport, *Chem. Mater.*, 120 (2000) 605-607.
- [73] A.M. Morales and C.M. Lieber, A laser ablation method for the synthesis of crystalline semiconductor nanowires, *Science* 279 (1998) 208-211.
- [74] M.K. Sunkara, S. Sharma, R. Miranda, G. Lian and E.C. Dickey, Bulk synthesis of silicon nanowires using a low-temperature vapor-liquid-solid method, *Appl. Phys. Lett.* 79 (2001) 1546-1548.
- [75] S. Sharma, M.K. Sunkara, R. Miranda, G. Lian and E.C. Dickey, A novel low temperature synthesis method for semiconductor nanowires. In: H.W. Hahn, D.L. Feldheim, C.P. Kubiak, R. Tannenbaum and R.W. Siegel (Eds.), *Synthesis, Functional Properties and Applications of Nanostructures*, Mater. Res. Soc. Symp. Proc., San Francisco, Spring 2001, Materials Research Society Press, Pittsburgh, PA, Vol. 676 (2001) Y1.6.
- [76] P.M. Parthangal, R.E. Cavichchi and M.R. Zachariah, A universal approach to electrically connecting nanowire arrays using nanoparticles: Application to a novel gas sensor architecture, *Nanotechnology* 17 (2006) 3786-3790.
- [77] M.S. Gudiksen, L.J. Lauhon, J. Wang, D.C. Smith, and C.M. Lieber, Growth of nanowire superlattice structures for nanoscale photonics and electronics, *Nature* 415 (2002) 617-620.
- [78] Y. Wu, R. Fan and P. Yang, Block-by-block growth of Si/SiGe superlattice nanowires, *Nano Lett.* 2 (2002) 83-86.
- [79] M.T. Bjork, B.J. Ohlsson, T. Sass, A.I. Persson, C. Thelander, M.H. Magnusson, K. Deppert, L.R. Wallenberg and L. Samuelson, One-dimensional steeplechase for electrons realized, *Nano Lett.* 2 (2002) 87-89.
- [80] N. Wang, Y.H. Tang, Y.F. Zhang, C.S. Lee and S.T. Lee, Nucleation and growth of Si nanowires from silicon oxide, *Phys. Rev. B* 58 (1998) R16024-R16026.
- [81] N. Wang, Y.F. Zhang, Y.H. Tang, C.S. Lee and S.T. Lee, SiO<sub>2</sub>-enhanced synthesis of Si nanowires by laser ablation, *Appl. Phys. Lett.* 73 (1998) 3902-3904.
- [82] Y.F. Zhang, Y.H. Tang, N. Wang, C.S. Lee, I. Bello and S.T. Lee, One-dimensional growth mechanism of crystalline silicon nanowires, *Journal of Crystal Growth* 197 (1999) 136-140.
- [83] Y.F. Zhang, Y.H. Tang, N. Wang, C.S. Lee, I. Bello and S.T. Lee, Germanium nanowires sheathed with an oxide layer, *Physical Review B* 61 (2000) 4518-4521.
- [84] S.T. Lee, Y.F. Zhang, N. Wang, Y.H. Tang, I. Bello, C.S. Lee and Y.W. Chung, Semiconductor nanowires from oxides, *J. Mater. Res.* 14 (1999) 4503-4507.

- [85] B. Gates, Y. Yin and Y. Xia, A solution-phase approach to the synthesis of uniform nanowires of crystalline selenium with lateral dimensions in the range of 10-30 nm, *J. Am. Chem. Soc.* 122 (2000) 12582-12583.
- [86] B. Gates, B. Mayers, B. Cattle and Y. Xia, Synthesis and characterization of uniform nanowires of trigonal selenium. *Adv. Funct. Mat.* 12 (2002) 219-227.
- [87] B. Mayers, B. Gates, Y. Yin and Y. Xia, Large-scale synthesis of monodisperse nanorods of Se/Te alloys through a homogeneous nucleation and solution growth process, *Adv. Mat.* 13 (2001) 1380-1384.
- [88] B. Gates, Y. Wu, Y. Yin, P. Yang and Y. Xia, Single-crystalline nanowires of  $\text{Ag}_2\text{Se}$  can be synthesized by templating against nanowires of trigonal Se, *J. Am. Chem. Soc.* 123 (2001) 11500-11501.
- [89] B. Gates, B. Mayers, Y. Wu, Y. Sun, B. Cattle, P. Yang and Y. Xia, Synthesis and characterization of crystalline  $\text{Ag}_2\text{Se}$  nanowires through a template-engaged reaction at room temperature, *Adv. Funct. Mat.* 12 (2002) 679-686.
- [90] C. A. Huber, T. E. Huber, M. Sadoqi, J. A. Lubin, S. Manalis and C. B. Prater, Nanowire array Composites, *Science* 263 (1994) 800-802.
- [91] Z. Zhang, J. Y. Ying and M. S. Dresselhaus, Bismuth quantum-wire arrays fabricated by a vacuum melting and pressure injection process, *J. Mater. Res.* 131 (1998) 1745-1748.
- [92] H.S. Virk, K. Kishore and V. Baloria, Fabrication of Copper Nanowires by Electrodeposition using Anodic Alumina and Polymer Templates. *J. of Nano Research* 10 (2010) 63-67.
- [93] H.S. Virk, Fabrication of polycrystalline copper nanowires by electrodeposition in anodic alumina membrane and their characterization, *Nano Trends* 9(1) (2010) 1-9.
- [94] J. Brotz, F. Maurer, T.W. Cornelius and M.E. Toimil Molares, Controlled deposition of Copper nanowires for field emission investigations, *Micro. Anal. in Mater. Sci. Freiberg*, 2005, pp. 1-3.
- [95] H. Cao, L. Wang, Y. Qiu and L. Zhang, Synthesis and I-V properties of aligned copper nanowires, *Nanotechnology* 17 (2006) 1736-1739.
- [96] G. Riveros, H. Gomez and E.A. Dalchiele, Electrochemical Growth of Copper Nanowires: Structure Properties, *Electrochim. Society* <http://www.electrochem.org/dl/ma/203/pdfs/1679.pdf>
- [97] T. Gao, G. Meng, Y. Wang, S. Sun and L. Zhang, Electrochemical synthesis of copper nanowires, *J. Phys.: Condens. Matter* 14 (2002) 355-363.
- [98] B.J. Hansen, G. Lu and J. Chen, Direct oxidation growth of  $\text{CuO}$  nanowires from Copper-containing substances, *J. of Nanomaterials*, 2008, doi:10.1155/2008/830474, pp. 1-7.
- [99] R. Ingunta, S. Piazza and C. Sunseri, Template electrosynthesis of aligned  $\text{Cu}_2\text{O}$  nanowires: Part I. abrication and characterization, *Electrochimica Acta* 53 (2008) 6504-6512.
- [100] C. Schonenberger, B. M. I. Vander Zande, L. G. J. Fokkink, M. Henry, C. Schmid, M. Kniger, A. Bachtold, R. Huher, H. Birk and V. Stairfer, Template synthesis of nanowires in porous polycarbonate membranes: Electrochemistry and Morphology, *J. Phys. Chem. B* 101 (1997) 5497-5505.
- [101] B. Hamrakulov, I.S. Kim, M.G. Lee, B.H. Park, Electrodeposited Ni, Fe, Co and Cu single and multilayer nanowire arrays on anodic aluminum oxide template, *Trans. Nonferrous Met. Soc. China* 19 (2009) 83-87.

- [102] M. Mikhaylova, M. Toprak, D.K. Kim, Y. Zhang and M. Muhammed, Nanowire formation by electrodeposition in modified nanoporous polycrystalline anodic alumina templates, Mater. Res. Soc. Symp. Proc. 704 (2002) W6.34.1-6.
- [103] L. Menon, M. Zeng, H. Zeng, D.J. Sellmyer and S. Bandyopadhyay, Size Dependent Magnetic Properties of Fe Nanowires, J. Electron. Mater. 29 (2000) 510-514.
- [104] S. Kumar, S. Kumar, R. Kumar and S.K. Chakarvarti, Morphological and magnetic characterization of electrodeposited cobalt nanowires, J. Mater. Sci. 39 (2004) 2951-2953.
- [105] C. Kong, Z. Hu, H. Zhao, Y. Yang, X. Shang, L. Ren and Y. Wang, Preparation of Ag nanowire array electrode by transplantation and its electrochemical activities, Int. J. Electrochem. Sci. 2 (2007) 133-140.
- [106] K. Nielsch, R. Wehrspohn, S.F.H. Kronmuller, J. Barthel, J. Kirschner and U. Gosele, Magnetic properties of 100 nm nickel nanowire arrays obtained from ordered porous alumina templates, MRS Symp. Proc. 636 (2001) D1.9 (1-6).
- [107] I.Z. Rahman, K.M. Razeeb, M.A. Rahman and Md. Kamruzzaman, Fabrication and Characterization of nickel nanowires deposited on metal substrate, J. Magn. & Magn. Mater. 262 (2003) 166-169.
- [108] T.M. Whitney, J.S. Jiang, P.C. Searson and C.L. Chien, Fabrication and magnetic properties of arrays of metallic nanowires, Science 261 (1993) 1316-1319.
- [109] P. Yang, H. Yan, S. Mao, R. Russo, J. Johnson, R. Saykally , N. Morris, J. Pham, R. He and H.J. Choi, Controlled growth of ZnO nanowires and their optical properties, Adv. Func. Mat. 12 (2002) 323-331.
- [110] X.J. Xu, G.T. Fei, W.H. Yu, X.W. Wang, L. Chen and L.D. Zhang, Preparation and formation mechanism of ZnS semiconductor nanowires made by the electrochemical deposition method, Nanotechnology 17 (2006) 426-429.
- [111] Y. Huang, X. Duan, Y. Cui and C.M. Lieber, Gallium nitride nanodevices, Nano Letters 2 (2002) 101-104.
- [112] H. S. Virk, Template synthesis and morphology of CdS nanowire arrays using anodic alumina membranes, Nano Trends 10 (2) (2011) 17-24.
- [113] S.P. Mondal, A. Dhar and S.K. Roy, Optical properties of CdS nanowires prepared by dc electro-chemical deposition in porous alumina template, Mater. Sci. in Semicond. Processing 10 (2007) 185-193.
- [114] G. Ghenescu, L. Ion, I. Enculescu, C. Tazlaoanu, V.A. Antohe, M. Sima, M. Enculescu, E. Matei, R. Neumann, O. Ghenescu, V. Covlea and S. Antohe, Electrical properties of electrodeposited CdS nanowires, Physica E 40 (2008) 2485-2488.
- [115] J. Milam, L. Lauhon and J. Allen, Photoconductivity of sSemiconducting CdS Nanowires, Nanoscape 2(1) 2005) 43-47.
- [116] D. Xu, Y. Xu, D. Chen, G. Guo, L. Gui and Y. Tang, Preparation and characterization of CdS nanowire arrays by dc electrodeposit in porous anodic aluminium oxide templates, Chem Phys. Lett. 325 (2000) 340-344.
- [117] Y. Yang, H. Chen, Y. Mei, J. Chen, X. Wu and X. Bao, Anodic alumina template on Au/Si substrate and preparation of CdS nanowires, Solid State Comm. 123 (2002) 279-282.
- [118] C. Ma, Y. Ding, D. Moore, X. Wang and Z.L. Wang, Single-Crystal CdSe Nanosaws, J. Am. Chem. Soc. 126 (2004) 708-709.

- [119] X.S. Peng, J. Zhang, X.F. Wang, Y.W. Wang, L.X. Zhao, G.W. Meng and L.D. Zhang, Synthesis of highly ordered CdSe nanowire arrays embedded in anodic alumina membrane by electrodeposition in ammonia alkaline solution, *Chem. Phys. Lett.* 343 (2001) 470-474.
- [120] R. Singh, R. Kumar and S.K. Chakarvarti, Non-galvanic template synthesis of CdSe nanowires using Anodic Alumina Membrane and their optical band gap determination, *Mater. Lett.* 62 (2008) 874-877.
- [121] S. Kumar, S. Kumar, N.K. Verma and S.K. Chakarvarti, Fabrication of CdSe nanowires using template synthesis technique, *J. Optoelectronics & Adv. Mater.* 9(10) (2007) 3191-3193.
- [122] S. Kumar, S. Kumar, N.K. Verma, S.K. Chakarvarti and J.K. Sharma, Electrochemical synthesis And laser induced time resolved luminescence behavior of CdSe nanowires, *Digest J. of nanomater. & Biostr.* 3(4) (2008) 199-202.
- [123] X.S. Peng, X.F. Wang, Y.W. Wang, C.Z. Wang, G.W. Meng and L.D. Zhang, Novel method synthesis of CdO nanowires, *J. Phys. D: Appl. Phys.* 35 (2002) L101-L104.
- [124] B. Xiang, H.Z. Zhang, G.H. Li, F.H. Yang, F.H. Su, R.M. Wang, J. Xu, G.W. Lu, X.C. Sun, Q. Zhao and D.P. Yu, Green-light-emitting ZnSe nanowires fabricated via vapor phase growth, *Appl. Phys. Lett.* 82 (2003) 3330-3333.
- [125] X. Duan, Y. Huang, Y. Cui, J. Wang and C.M. Lieber, Indium phosphide nanowires as building blocks for nanoscale electronic and optoelectronic devices. *Nature*, 409 (2001) 66-69.
- [126] X. Duan, J. Wang and C.M. Lieber, Synthesis and optical properties of gallium arsenide nanowires, *Appl. Phys. Lett.* 76 (2000) 1116-1118.
- [127] S. Kumar, Synthesis and characterization of Selenium nanowires using template synthesis, *J. Experimental Nanosci.* 4(4) (2009) 341-346.
- [128] H.Y. Chao, J.H. Cheng, J.Y. Lu, Y.H. Chang, C.L. Cheng and Y.F. Chen, Growth and characterization of type-II ZnO/ZnTe core-shell nanowire arrays for solar cell applications, *Superlattices and Microstructures* 47 (1) (2010) 160-164.
- [129] Y. Leprince-Wang, G.Y. Wang, X.Z. Zhang and D.P. Yu, Study on the microstructure and growth mechanism of electrochemical deposited ZnO nanowires, *Journal of Crystal Growth* 287 (1) (2006) 89-93.
- [130] M. Chaudhari, A. Vohra, S.K. Chakarvarti and R. Kumar, Template synthesized Cu-Se microstructures as resonant tunneling diodes, *J. Mater. Sci.: Mater. Electron* 17 (2006) 189-192.
- [131] R. Singh, R. Kumar and S.K. Chakarvarti, Size effect on I-V characteristics of low dimensional metal-semiconductor heterojunctions, *Physica E* 40 (2008) 591-593.
- [132] M. Chaudhari, A. Vohra and S.K. Chakarvarti, Thermal annealing effects on Cu-Se resonant tunneling diodes fabricated by electrodeposition-assisted template synthesis technique, *Mater. Sci. & Engg. B* 149 (2008) 7-11.
- [133] H.S. Virk, Template synthesis of Cu-Se heterojunctions using anodic alumina membrane and their characterization, *Digest J. Nanomater. & Biostruc.* 5(3) (2010) 593-598.
- [134] R. Kumar, M. Chaudhari and S.K. Chakarvarti, Morphology and collective I-V characteristics of template synthesized nano metal-semiconductor heterojunctions, *Mater. Letters* 61 (2007) 1580-1582.
- [135] M. Chaudhari, A. Vohra and S.K. Chakarvarti, Fabrication of Zn/Cd-Se micro heterostructures by electrochemical deposition in the pores of polycarbonate track-etch membranes and their characterization, *Physica E* 40 (2008) 849-851.

- [136] M.T. Bjork, B.J. Ohlsson, C. Thelander, A.I. Persson, K. Deppert, L.R. Wallenberg and L. Samuelson, Nanowire resonant tunneling diodes, *Appl. Phys. Lett.* 81 (2002) 4458-4460.
- [137] G.B. Ji, W. Chen, S.L. Tang, B.X. Gu, Z. Li and Y.W. Du, Fabrication and magnetic properties of ordered 20 nm Co-Pb nanowire arrays, *Solid State Comm.* 130 (2004) 541-545.
- [138] Saedi and M. Ghorbani, Electrodeposition of Ni-Fe-Co alloy nanowire in modified AAO template, *Mater. Chem. & Phys.* 91 (2005) 417-423.
- [139] L. Menon, Synthesis of Nanowires using Porous Alumina, in: Hari Singh Nalwa and S. Bandhopadhyaya (Eds.), *Quantum Dots and Nanowires*, American Scientific Publishers, Cal. USA, 2003, pp. 142-187.
- [140] D.B. Cullity, *Elements of X-ray Diffraction*, Addison-Wesley Inc. Massachusetts, USA, 1956.
- [141] H. Mehrez and H. Guo, *Nanowires and Nanotubes--Materials, Properties and Devices*, Vol. I: Metal and Semiconductor Nanowires, (Ed.) Z. L. Wang, Tsinghua University Press, Beijing, 2004, pp. 95–124.
- [142] J.W.G. Wildoer, L.C. Venema, A.G. Rinzler, R.E. Smalley and C. Dekker, Electronic structure of atomically resolved Carbon nanotubes, *Nature* 391 (1998) 59-62.
- [143] K. Itakura, Y. Yuki, S. Kurokawa, H. Yasuda and A. Sakai, Bias dependence of the conductance of Au nanocontacts, *Phys. Rev. B* 60 (1999) 11163- 11170.
- [144] S. Manna, S. Das, S.P. Mondal, R. Singha and S.K. Ray, High Efficiency Si/CdS Radial Nanowire Heterojunction Photodetectors Using Etched Si Nanowire Templates, *J. Phys. Chem. C*, 116 (12) (2012) 7126–7133.
- [145] Y. Huang and C.M. Lieber, Integrated nanoscale electronics and optoelectronics: Exploring nanoscale science and technology through semiconductor nanowires, *Pure Appl. Chem.* 76(12) (2004) 2051– 2068.
- [146] X. Duan and Y. Huang, Chemically Synthesized Semiconductor Nanowires for High-Performance Electronics and Optoelectronics, Chapter 2, in: Y. Sun and J.A. Rogers (Eds.), *Semiconductor Nanomaterials for Flexible Technologies*, Elsevier, UK, 2010, pp. 27-62.
- [147] W. Yang, Z. Wu, Z. Lu, X. Yang and L. Song, Template-electrodeposition preparation and Structural properties of CdS nanowire arrays, *Microelect. Eng.* 83 (2006) 1971–1974.
- [148] D. Xu, Y. Xu, D. Chen, G. Guo, L. Gui and Y. Tang, Preparation and Characterization of CdS Nanowire Arrays by DC Electrodeposit in Porous Aluminum Oxide Templates, *Chem. Phys. Letters*, 325 (2000) 340-344.
- [149] L. Sun, R.L. Zong, S.K. Shi and J. Zhou, Synthesis of Sulfide Nanowire Arrays through Template-Assisted Electrodeposition, *Key Eng. Mater.* 336–338 (2007) 2163–2165.
- [150] C.M. Leiber and Z.L. Wang, Functional Nanowires, *MRS Bull.* 32 (2) (2007) 99-108.
- [151] A.R. Rathmell, S. M. Bergin, Y. L. Hua, Z-Y. Li and B.J. Wiley, The growth mechanism of copper nanowires and their properties in flexible, transparent conducting films. *Adv. Mater.* 22 (2010) 3558- 3563.
- [152] Y. Chang, M. L. Lye and H. C. Zeng, Large-scale synthesis of high-quality ultralong copper nanowires, *Langmuir* 21 (2005) 3746-3748.
- [153] T. Daff , I. Saadoune , I. Lisiecki and N. Leeuw, Computer simulations of the effect of atomic structure and coordination on the stabilities and melting behaviour of copper surfaces and nano-particles, *Surf. Sci.* 603 (2009) 445-454.
- [154] M. I. Baskes, Modified Embedded-Atom Potentials for Cubic Materials and Impurities, *Phys. Rev. B* 46 (1992) 2727-2742.

- 
- [155] Galanakis, N. Papanikolaou and P.H. Dederichs, Applicability of the Broken- Bond Rule to the Surface Energy of the fcc Metals, *Surf. Sci.* 511 (2002) 1-12.
  - [156] J. Ahn, H. Kim, K. Lee, S. Jeon, S. Kang, Y. Sun, R. Nuzzo and J. Rogers, Heterogeneous Three Dimensional Electronics Using Printed Semiconductor Nanomaterials, *Science* 314 (2006) 1754-1757.
  - [157] C. O'Dwyer, M. Szachowicz, G. Visimberga, V. Lavayen, S. Newcomb, C. Torres, M. Sotomayor, Bottom-up growth of fully transparent contact layers of indium tin oxide nanowires for light-Emitting- devices, *Nature Nanotech.* 4 (2009) 239-244.
  - [158] R. G. Gordon, Criteria for Choosing Transparent Conductors, *MRS Bull.* 25-57(2000) 52-57.

**Functional Nanomaterials and their Applications**

10.4028/www.scientific.net/SSP.201

**Synthesis and Characterization of Metal and Semiconductor Nanowires**

10.4028/www.scientific.net/SSP.201.21